MAGNETIZATION UNITS

GL02155 from USGS OFR-85-459

Also see OFR-85-49 Rosenbaum & Snyder

OBSERVED, RESIDUAL, AND SMOOTHED ANOMALIES

The observed data recorded by a magnetometer during an aeromagnetic or ground magnetic survey consist of the anomalies from the geologic features being studied plus the combined effects of the undisturbed geomagnetic field, magnetized sources deep within the Earth's crust, and man-made objects near the surface. Residual anomalies are those that remain after the Earth's field and effects of deep sources and man-made objects are removed from the observed data. The change in the Earth's field was eliminated from aeromagnetic data by removing the International Geomagnetic Reference Field (Barraclough and Fabiano, 1978), and from ground magnetic data by removing increases of 5.64 nT/km northward and 1.72 nT/km eastward. Effects of deep crustal sources were mostly eliminated by adjustment of observed data to an assumed zero field near Mercury in the southeastern corner of the Nevada Test Site (Bath and others, 1983). The zero field is the average value measured over a large area of nonmagnetic sedimentary rocks that are assumed to extend to great depths. Observed ground anomalies in areas near drill casing and other iron and steel objects are considered unreliable and therefore omitted from the data.

Residual anomalies were compiled for four air traverses and five ground traverses in the vicinity of the prominent aeromagnetic anomaly, and locations of traverses are given on the topographic map of figure 2. Figure 3 gives continuous measurements of anomalies and altimeter records for air traverses A, B, C, and D located on figures 1 and 2. The prominent anomaly is on traverse B. Ground anomalies were measured at 3-m (10-ft) intervals and are shown on figure 4 for traverse A82, figure 5 for traverse A83, figure 6 for traverse B83, and figure 7 for traverse C83. Ground traverse H82 is shown by Bath and Jahren (1984) on their figure 20. Ground anomalies measured close to magnetized rock have very irregular shapes, and a severe method of smoothing was used to convert them to a form resembling air anomalies. Each traverse was smoothed by continuation upward 122 m (400 ft) by the method of Henderson and Zietz (1949), and the resulting values were multiplied by a constant to restore the average value at ground level.

MAGNETIC PROPERTIES

The average total magnetization of a uniformaly magnetized rock mass, denoted as the vector $\vec{J}_t$ is defined as the vector sum of the induced magnetization, $\vec{J}_i$, and remanent magnetization, $\vec{J}_r$:

$$\vec{J}_t = \vec{J}_i + \vec{J}_r$$

Air and ground magnetic surveys will commonly detect an ash or lava flow when its average total magnetization is equal to or greater than 0.05 A/m (Bath, 1968). Therefore, units having intensities less than 0.05 A/m are herein designated nonmagnetic; and those having greater intensities are herein arbitrarily designated as either weakly, moderately, or strongly magnetized as defined by the following limits:

nonmagnetic $\leq$ 0.05 A/m

0.05 A/m < weakly magnetized < 0.50 A/m

0.50 A/m < moderately magnetized < 1.50 A/m

1.50 A/m < strongly magnetized

Total magnetizations varying from nonmagnetic to strongly magnetic and of both normal and reversed polarities, were found in drill core samples from geologic exploration holes and surface samples in the Yucca Mountain area Rosenbaum and Snyder, 1985). Large changes in magnetic intensity occur both laterally and vertically within the volcanic ash-flow sheets. Average magnetizations were determined for units mapped by Lipman and McKay (1965) and Scott and Bonk (1984), and penetrated in drill holes USW G-1 (Spengler and others, 1981), USW G-2 (Maldonado and Koether, 1983), and USW G-3 and USW GU-3 (Scott and Castellanos, 1984). The magnetic intensity values suggest the following eight units as possible anomaly producers in the vicinity of major faults in the Yucca Mountain area:

Rainier Mesa Member of the Timber Mountain Tuff (Tmr)
Tiva Canyon Member of the Paintbrush Tuff (Tpc)
Pah Canyon Member of the Paintbrush Tuff (Tpp)
Topopah Spring Member of the Paintbrush Tuff (Tpt)
Bullfrog Member of the Crater Flat Tuff (Tcb)
Tram Member of the Crater Flat Tuff (Tct)
Lava flow and flow breccia (Tfb)Lava and flow breccia (Tll)

Considerations of thicknesses, and lateral extent of units has narrowed the eight to the Tiva Canyon, Topopah Spring, Bullfrog, and Tram Members. Their average magnetic properties and thicknesses are given in table 1. Modelling studies by Bath and Jahren (1984) showed a close resemblance between observed aeromagnetic anomalies in the Yucca Mountain area and theoretical anomalies computed for the faulted Topopah Spring Member. Their study designated the Topopah Spring Member as the most likely primary source of aeromagnetic anomalies.

Estimate of Magnetization

The method of estimating total magnetization by Smith (1961, equation 2.7) has been modified and applied to ground magnetic anomalies arising from near surface rocks in the NTS area by Bath and others (1983) and Bath and Jahren (1984). The estimates are based on the irregular and abrupt changes in anomaly amplitudes and shapes found in many ground traverses, and on the method of estimating depths to anomaly sources by Vacquier and others (1951). It is thus possible to use anomaly amplitudes to give minimum estimates of total magnetization within the following limits:

nonmagnetic $\leq$ 15 nT

15 nT < weakly magnetized < 150 nT

150 nT < moderately magnetized < 450 nT

450 nT < strongly magnetized

Table 1.--Magnetic properties and thicknesses of four units that were penetrated in three holes drilled on Yucca Mountain. These are the most likely sources of magnetic anomalies

Unit	Drill hole	Magnetic polarity	J_t (A/m)	Thickness (m)	Comments
Tpc	USW G-3	Reversed	0.9	103	Entire unit
Tpt	USW G-1	Normal	1.3	335	Entire unit
Do.	do.	do.	0.7	169	upper part
Do.	do.	do.	2.0	166	lower part
Do.	USW G-2	do.	1.4	285	Entire unit
Do.	do.	do.	0.7	102	upper part
Do.	do.	do.	1.7	183	lower part
Do.	USW G-3	do.	1.2	272	Entire unit
			1.3	297	Average for entire unit
Tcb	USW G-1	Normal	1.0	130	Entire unit
Do.	USW G-2	do.	0.2	128	Entire unit (altered)
Do.	USW G-3	do.	3.0	182	Entire unit
			1.4	147	Average for entire unit
Tct	USW G-1	Reversed	1.2	268	Entire unit
Do.	do.	do.	2.0	142	upper part
Do.	do.	do.	0.1	126	lower part (altered)
Do.	USW G-2	do.	0.2	128	Entire unit (altered)
Do.	USW G-3	do.	1.8	369	Entire unit
			1.1	255	Average for entire unit

USGS-OFR-94-413-A

U.S. Department of the Interior
U.S. Geological Survey

Gravity and magnetic data across the Ghost Dance Fault in WT-2 Wash, Yucca Mountain, Nevada

by

H.W. Oliver and R.F. Sikora

U.S. Open-File Report 94-413-A

Prepared in cooperation with the Nevada Field Office
U.S. Department of Energy
(Interagency Agreement DE-AI08-92NV10874)

Menlo Park, California
1994

U.S. DEPARTMENT OF THE INTERIOR

BRUCE BABBITT, Secretary

U.S. GEOLOGICAL SURVEY

Gordon P. Eaton, Director

For additional information write to:

Chief, Geologic Studies Program
Yucca Mountain Project Branch
U.S. Geological Survey
Box 25046, MS 421
Denver Federal Center
Denver, CO 80225

Copies of this report can be purchased from:

U.S. Geological Survey
Earth Science Information Center
Open-File Reports Section
Box 25286, MS 517
Denver Federal Center
Denver, CO 80225

Tables of Contents

Tables

Illustrations

Units, Conversion Factors, and Vertical Datum

All elevation and distance measurements in this report are in feet (ft) or miles (mi), because that is the unit used by the LBL surveyors.

Multiply	By	To obtain
feet (ft)	0.3048	meter (m)
mile (m)	1.609	kilometer (km)
square mile (mi^2)	2.590	square kilometer (km2)

Sea level: In this report "sea level" refers to the National Geodetic Vertical Datum of 1929 (NOVD of 1929)—a geodetic datum derived from a general adjustment of the first-order level nets of both the United States and Canada, formerly called Sea Level Datum of 1929.

Gravity measurements are in milligals (mGal)

$$1 \text{ mGal} = 10^{-3} \text{ cm/sec}^2 \text{ (acceleration)}$$
$$= 10^{-3} \text{ dyne/gram mass (force)}$$

Magnetic measurements are in nanoteslas (nT)

$$1 \text{ nT} = 1 \gamma \text{ (gamma)} = 10^{-5} \text{ gauss}$$

Remanent magnetization measurements are in amperes per meter (Am^{-1})

$$1 \text{ Am}^{-1} = 10^{-3} \text{ emu/cm}^3$$

For additional information on conversion factors between English (fps), metric (cgs), and the International System (SI) units, see U.S. National Bureau of Standards (1977).

Abstract

Detailed gravity and ground magnetic data were obtained in September 1993 along a 4650 ft-long profile across the Ghost Dance Fault system in WT-2 Wash. Gravity stations were established every 150 feet along the profile. Total-field magnetic measurements made initially every 50 ft along the profile, then remade every 20 ft through the fault zone. These new data are part of a geologic and geophysical study of the Ghost Dance Fault (GDF) which includes detailed geologic mapping, seismic reflection, and some drilling including geologic and geophysical logging. The Ghost Dance Fault is the only through-going fault that has been identified within the potential repository for high-level radioactive waste at Yucca Mountain, Nevada.

Preliminary gravity results show a distinct decrease of 0.1 to 0.2 mGal over a 600-ft-wide zone to the east of and including the mapped fault. The gravity decrease probably marks a zone of brecciation. Another fault-offset located about 2000 ft to the east of the GDF was detected by seismic reflection data and is also marked by a distinct gravity low.

The ground magnetic data show a 200-ft-wide magnetic low of about 400 nT centered about 100 ft east of the Ghost Dance Fault. The magnetic low probably marks a zone of brecciation within the normally polarized Topopah Spring Tuff, the top of which is about 170 ft below the surface, and which is known from drilling to extend to a depth of about 1700 ft. Three-component magnetometer logging in drill hole WT-2 located about 2700 ft east of the Ghost Dance Fault shows that the Topopah Spring Tuff is strongly polarized

magnetically in this area, so that fault brecciation of a vertical zone within the Tuff could provide an average negative magnetic contrast of the 4 Am^{-1} needed to produce the 400-nT low observed at the surface.

Additional magnetic data and limited gravity data are needed to determine the north-south extent of the geophysical anomalies and to better define the rather striking anomalies discovered in this initial survey.

Introduction

A gravity and magnetic investigation of the Ghost Dance Fault was begun as part of an effort to help geologically characterize Yucca Mountain as a potential site for the storage of commercial spent nuclear fuel and high-level radioactive waste. The Ghost Dance Fault is considered one of the more important structural features, as it is the only through-going fault that has been identified within the proposed repository area (Spengler and others, 1993; see fig. 1, this report). Seismic reflection, vertical seismic profiling (VSP), and cross-hole seismic profiling data are also being obtained across the Ghost Dance Fault by the Lawrence Berkeley Laboratory (LBL) in conjunction with this study (Majer and Karageorgi, 1994).

Acknowledgments

Dr. Cameron Ainsworth assisted with the staking and both the gravity and ground magnetic field measurements in September 1993. E.L. Majer and his coworkers at LBL surveyed in all of our gravity stations, and they used them

also for their seismic control. Elaine Ezra of EG & G, Las Vegas, compiled a new 1:6,000-scale topographic map of the immediate area of WT-2 Wash (EG&G, 1993) which proved invaluable for plotting our data points and making inner-zone terrain corrections to our gravity data.

General Geology and Drill Holes

Miocene volcanic tuffs make up the geologic section in the potential repository area and their stratigraphy and nomenclature has been recently revised by Sawyer and others (in press). The Tiva Canyon Tuff crops out over most of the area and has an age of 12.7 Ma (Hudson and others, 1994, table 1). This tuff is underlain by the two thin units (generally less than 100 ft thick) known as the Yucca Mountain and Pah Canyon Tuffs, and these tuffs are underlain by the 12.8 Ma Topopah Spring Tuff. Within the WT-2 Wash area, drilling in WT-2, UZ-7, and WT-2 (figs. 2 and 3) and geologic mapping have established that the thickness of the Tiva Canyon Tuff there ranges from about 160 ft at UZ-7 to 260 ft at WT-2. The Tiva Canyon Tuff is underlain by only 10 to 20 ft of Yucca Mountain and Pah Canyon Tuffs. The Topopah Spring Tuff was found to be about 1000 ft thick in both well WT-2 and WT-2 (R.W. Spengler, personal commun., 1994). The top of the Topopah Spring Tuff is a very important boundary magnetically, because it represents the bottom of reversely polarized volcanic strata in the WT-2 Wash area.

Structurally, Yucca Mountain consists of a series of north-trending, east-tilted, 0.6- to 2.5-mi wide structural blocks bounded by north-trending westward-dipping, high-angle faults (U.S. Geological Survey, 1984). The

Ghost Dance Fault is one of these north-trending faults (fig. 1) and is thought to displace volcanic strata by about 100 ft in the WT-2 Wash area. Detailed mapping by Spengler and others (1993) indicates that the Ghost Dance Fault is not a single fault but "represents the major fault within a previously unrecognized zone of minor faults, fractured rock, and stratal flexing that extends over a width of at least 700 ft."

Gravity Data

Gravity data were collected at stations spaced 150 ft apart along profile A-A' across the Ghost Dance Fault (fig. 2) using LaCoste and Romberg gravity meter G17C. Gravity-meter performance and calibration factors were checked in March 1993 over the Mt. Hamilton gravity meter calibration loop in California (Barnes and others, 1969), and its performance qualifies under USGS Technical Procedure GPP-01, Rev. 2, Gravity Methods (1991). Gravity data were reduced using the Geodetic Reference System of 1967 (International Union of Geodesy and Geophysics, 1971) and referenced to the International Gravity Standardization Net 1971 gravity datum (Morelli, 1974, p. 18) via base station MERC at the USGS core library building at Mercury, Nevada (Ponce and Oliver, 1981, p. 13). Because of recent building construction near base station MERC, the gravity value there now has a new value of 979,518.91 mGal, determined by repeated ties to nearby station TCCA, which is located on basement rocks (D.A. Ponce, written commun., 1993).

Gravity stations were surveyed using an electronic-distance-measurement instrument, and station elevations are accurate to within about 0.1 ft relative to a reference bench mark. Terrain corrections were computed to a radial distance of 104 mi and involved a 3-part process: (1) Hayford-Bowie zones A and B with an outer radius of 223 ft were estimated in the field with the aid of tables and charts, or sketched and later calculated in the office, (2) Hayford-Bowie zones C and D with an outer radius of 1935 ft were calculated by averaging compartment elevations on a circular template based on Hayford's system of zones (Swick, 1942, p. 66), and (3) terrain corrections from a distance of 0.37 mi to 104 mi were calculated using a digital elevation model and a procedure by Plouff (1977). Small amplitude errors in some of the profiles may be related to small errors in the terrain corrections, particularly where profiles cross topographic features such as hills. Gravity data were reduced to complete Bouguer anomalies using reduction densities of 1.6, 1.8, 2.0. 2.2, 2.4, and 2.67 g/cm^3, and include earth-tide, instrument drift, free-air, Bouguer, latitude, curvature, and terrain corrections.

In general, the observed gravity data are accurate to about 0.03 mGal, and the Bouguer anomalies are accurate to about 0.1 mGal. Principal facts of the gravity data are listed in table 1, and the data are plotted along profile A-A' in figure 3. The smoothness of the profiled data, particularly in the interval between G10 and G19, suggests that the relative accuracy of the Bouguer anomalies in this area may be good to ±0.05 mGal, although the single-station gravity high at station G102 may indicate that Bouguer anomalies at this station could be too high by about 0.15 mGal. The terrain correction for zones A-D for this station is the largest of all stations (1.23 mGal), and large

terrain corrections cause greater uncertainties, perhaps as much as 0.2 mGal in this case.

Density Data

No new density data were obtained from the WT-2 Wash area. However, Snyder and Carr (1984, table 1) report an average value of 2.1 g/cm^3 for the density of the Tiva Canyon Tuff; this tuff forms most of the topography in the study area. Study of the variations in Bouguer anomalies (fig. 3) suggests that a reduction density of 2.0 g/cm^3 provides the flattest curve over the western third of the profile (between G103 to G10); the 2.0 g/cm^3 curve in this interval is therefore independent of the eastward drop-off in elevation shown on the elevation profile. The eastern two-thirds of the profile (G11-G12) shows an eastward increase in gravity for all densities, and this regional gravity rise is known to be caused by an eastward rise in Paleozoic basement rocks in precisely this area (Oliver and Fox, 1993; Oliver and Ponce, in press; Oliver and Mooney, 1992).

Magnetic Data

Ground magnetic data were obtained along profile A-A' (table 2, fig. 4). A Geometrics portable proton precession magnetometer model G-816 was used to collect data with the sensor 8 ft above the surface. The whole 4650 ft-long profile was initially measured at 50-ft intervals, and later repeated between G4 and G8 across the Ghost Dance Fault with a reduced spacing of about 20 ft.

A three-component magnetometer log of drill hole WT-2 was made to a depth of about 1640 ft by P.H. Nelson (written commun., 1994). These new data confirm that magnetically reversely polarized strata extend from the surface to a depth of 230 ft, below which the strata (the Topopah Spring Tuff) are normally magnetized to a depth of about 1700 ft. For perspective, the magnetic stratigraphy at Yucca Mountain is summarized by Oliver and others (1990, Table 2.2-2).

For a regional perspective of the magnetic field within and surrounding the potential repository, see Oliver and others (1991, fig. 3) and Kirchoff-Stein and others (1989).

Preliminary Results

The gravity data plots do not indicate any striking anomalies along A-A', but a distinct decrease of about 0.2 mGal at G5 corresponds with the mapped location of the Ghost Dance Fault. Relative to the regional trend shown as dashed lines on the 2.0 and 2.2 g/cm^3 curves (fig. 3), the 0.2-mGal decrease seems to extend from G5 to G9 and may mark a zone about 600 ft wide of relatively low-density fault breccia. Similarly, another fault with a vertical displacement of about 70 ft near G20 (Majer and Karageorgi, 1994) is also marked by a 0.15-mGal local gravity low. However, a similar fault near G16 does not have a corresponding gravity low or offset.

By contrast, the ground magnetic data plot (fig. 4) shows striking anomalies associated not only with the Ghost Dance Fault but with the other two faults as well. The Ghost Dance Fault anomaly consists of a magnetic low of nearly 400 nT centered only 20 ft east of the projected fault location, with broader magnetic highs of about 200 nT both east and west of the low. The magnetic low is about 200 ft wide, implying an approximate 200 ft wide source zone at the fault. The high to the west is somewhat questionable because the survey line passed about 80 ft south of drill hole UZ-8, which contains a 35-ft deep, 8-in-diameter metal casing. We did not know about this cased hole at the time of our measurements and need to run a N-S profile through UZ-8 to determine the lateral extent of its magnetic effect. However, cased holes typically have only a magnetic high or magnetic low signature and are not bipolar (Frischknecht and others, 1985). Hence, the 400-nT magnetic low at the Ghost Dance fault is not an artifact of the UZ-8 casing but a significant finding and agrees with Bath and Jahren's (1984, fig. 21) finding of a similar magnetic low associated with the Ghost Dance Fault in a truck-mounted-magnetometer profile in the next canyon to the north (fig. 1). Modeling of these magnetic lows is complicated by the fact that the approximate upper 200 ft of earth materials along the whole profile are composed of the reversely polarized Tiva Canyon Tuff with very strong, reversed-polarity, remanent magnetizations in the range of 1 to 6 Am^{-1} in the lower part of the formation (Rosenbaum and Snyder, 1985).

The presence of magnetic rocks in the valley walls above profile A-A' makes the interpretation and modeling of the magnetic profile more difficult (Rasmussen and Pedersen, 1979). However, a comparison of the magnetic

anomaly locations (fig. 4) with the proximity to side walls of WT-2 Wash (fig. 2) shows that the local anomalies are virtually independent of this possible problem. For example, the approximately 300-nT eastward rise in the magnetic field between G26 and G27 (fig. 4) occurs in a nearly flat portion of the wash where the sidewalls are gentle (less than 10°) and start rising about 500 ft (150 m) to the north and south of the profile. Thus, this magnetic anomaly must reflect subsurface magnetic structure. A more general westward increase in the magnetic field strength from about 50,950 nT near G14 to about 51,200 nT near G9 (fig. 4) does correlate with a narrowing of WT-2 Wash (fig. 2). However, further narrowing of this wash west of WT-2 does not produce a magnetic rise. Certainly, the sharp magnetic low of over 400 nT near the Ghost Dance Fault is not significantly affected by proximity to the valley walls of WT-2 Wash.

Some modeling of possible sources of the 400 nT magnetic low has been carried out, but nothing tried so far is completely satisfactory. The most promising model is a 200-ft-wide tabular body which may represent a loss of magnetic remanence within the fault zone that penetrates the normally polarized Topopah Spring Tuff. By assuming an average value of magnetization of 4 Am^{-1} for the Topopah Spring Tuff, the magnetic low can be fit rather well. However, brecciation of the upper 160 to 200 ft of Tiva Canyon Tuff would produce a sharper high superimposed on the modeled low, and a significant magnetic high is not observed. There is a sharp 100-nT blip located about 100 ft east of G5 within the 400-nT low that perhaps could be modeled if additional detailed magnetic data became available. Such

modeling might show the nature and extent of breciation associated with the Ghost Dance Fault within the Tiva Canyon Tuff.

Another possible source for the magnetic low associated with the Ghost Dance Fault is a tabular body within the fault zone with a greater reversed polarization than the Tiva Canyon Tuff. A dike-like model with a contrast of 4 Am^{-1} has been tested (Oliver and others, 1993), but there is no geologic evidence for such a body at present. The top of the modeled body is about 30 ft below the surface.

Conclusions and Recommendations

Ground magnetic measurements combined with limited gravity data offer considerable promise for inexpensively tracing the Ghost Dance Fault under alluvial cover and determining the lateral extent of faulting within the system.

To further facilitate this work, two short magnetic lines should be run at right angles across all of the drill holes within 200 ft of A-A' that are known to have steel casing to determine possible effects on the magnetic profile (fig. 4). The most important such well is UZ-8, only 80 ft to the north of the profile at G4082, where the highest magnetic measurement of 51223 nT was measured (table 2). Other such wells include WT-2, WT-2, UZ-N48, UZ-7, UZ-N50, and UZ-N56. Information on the depth, size, and type of casing needs to be compiled for all these wells. We also recommend obtaining density and magnetic logs for these wells as well as making systematic

magnetic susceptibility and remanent magnetization measurements of core samples. A magnetic log is available for UZ-16 (P.H. Nelson, written commun., 1994) which would be very helpful to this study.

Additional ground magnetic measurements are recommended for the following areas: (1) west of A along WT-2 Wash so as to extend the current survey about 1000 ft to the west and make it coincide exactly with the seismic reflection survey (Majer and Karageorgi, 1994); (2) across the Ghost Dance Fault (GDF) in "H4 Wash" to the north of Whale Back Ridge to check out the GDF magnetic signature reported by Bath and Jahren (1984); and (3) along Whale Back Ridge where the magnetic effect of the GDF will be free from possible sidewall effects. About five detailed ground magnetic profiles spaced about 20 ft apart should also be obtained both to the north and south of that portion of A-A' between G3 and G10 to test the N-S continuity of the 400 nT magnetic low associated with the Ghost Dance Fault measured along A-A' (fig. 4). Someone should also look at the canyon walls, making simple fluxgate polarity checks to see where the profile is relative to magnetic stratigraphy.

Because of the possibility of a reversely polarized tabular body within the GDF zone, detailed geologic inspection of the zone and shallow drilling of the magnetic low might provide important information to help characterize the area. Ground magnetic surveys should also be run across any other faults within Yucca Mountain that are known to contain tabular intrusive bodies such as the basaltic dike in the Solitario Canyon Fault (U.S. Geological Survey, 1984, p. 29).

It would also be helpful to obtain ground magnetic data across the southern extension of the Ghost Dance fault in Abandoned Wash (fig. 1). In this area, the Tiva Canyon Tuff has been eroded and the normally polarized Topopah Spring Tuff is exposed at the surface. Thus, the fault breccia model should produce a simple magnetic low in this area, uncontaminated by any reversely polarizing effects.

Electrical studies in the area of Drill Hole Wash (fig. 1) by Hoover (1982), Smith and Ross (1982), and D.P. Klein and Ernie Hardin (written commun., 1994) suggest that some fault zones at Yucca Mountain have a lower resistivity because of percolation of water through the opening. Also, the long-term effect of percolation has caused alteration of at least some fault zones and has produced a lower resistivity within the zone. Thus, resistivity and induced polarization measurements should also be considered for further studies of the Ghost Dance Fault zone.

Description of diskette

The data described in this report (tables 1 and 2) are available on 3 1/2-in, high-density, double-sided diskette formatted for Macintosh computer using Microsoft Word ~~(Oliver and Sikora, 1994)~~ WCH 9/27/94. The diskette requires a Macintosh computer/word processor and contains a total of four files:

(1) Title Page

(2) Read Me, a description of the gravity and magnetic data along

profile A-A'

(3) Table 1, principal facts of gravity stations along profile A-A'

(4) Table 2, Ground magnetic data along profile A-A'

References

Bath, G.D., and Jahren, C.E., 1984, Interpretations of magnetic anomalies at a potential repository site located in the Yucca Mountain area, Nevada Test Site: U.S. Geological Survey Open-File Report 84-120, 40 p. + 4 plates.

EG & G, 1993, Yucca Mountain repository topographic base map, sheet B: EG & G Map, Yucca Mountain Project 93-203.2, scale 1:6,000.

Frischknecht, F.C., Grette, R., Raab, P.V., and Meredith, J., 1985, Location of abandoned wells by magnetic surveys: Acquisition and interpretation of aeromagnetic data for five test areas: U.S. Geological Survey Open-File Report 85-614A, 64 p.

Hoover, D.B., Chornack, M.P., and Broker, M.M., 1982, E-Field ratio telluric traverses near Fortymile Wash, Nevada Test Site, Nevada: U.S. Geological Survey Open-File Report 82-1042, 14 p.

Hudson, M.R., Sawyer, D.A., and Warren, R.G., 1994, Paleomagnetism and rotation constraints for the middle Miocene southwestern Nevada volcanic field: Tectonics, v. 13, no. 2, p. 258-274.

International Union of Geodesy and Geophysics. 1971, Geodetic Reference System 1967: International Association of Geodesy Special Publication No. 3, 116 p.

Kirchoff-Stein, K.S., Ponce, D.A., and Chuchel, B.A., 1989, Preliminary aeromagnetic map of the Nevada Test Site and vicinity: U.S. Geological Survey Open-File Report 89-446, scale 1:100,000.

Majer, E.L., and Karageorgi, Eleni, 1994, Ghost Dance surface reflection profiles: DOE-YMSCO, YMP-USGS Rock Characteristics-/Lawrence Berkeley Laboratory Milestone Report 3GGF240M, 16 p.

Morelli, C., (Ed.), 1974, The International Gravity Standardization Net, 1971: International Association of Geodesy Special Publication No. 4, 194 p.

Oliver, H.W., and Fox, K.F., 1993, Structure of Crater Flat and Yucca Mountain, southeastern Nevada, as inferred from gravity data: American Nuclear Society Proceedings of the Fourth Annual International Conference on High Level Waste Management, v. 2, p. 1812-1817.

Oliver, H.W., Hardin, E.L., and Nelson, P.H., eds., 1990, Status of data, major results, and plans for geophysical activities, Yucca Mountain Project: U.S. Department of Energy Report YMP/90-38, 236 p.

Oliver, H.W., Majer, E.L., and Spengler, R.W., 1994, Geophysical investigations of the Ghost Dance fault, Yucca Mountain, Nevada (Abs):

Geological Society of America Cordilleran Section Meetings, San Bernardino, CA, March 21-23, 1994, Abstracts with Programs, p. 78.

Oliver, H.W., and Mooney, W.D., 1992, Characterizing Yucca Mountain, Nevada, by geophysical methods (Extended Abstract): American Geophysical Union 1992 Fall Meeting Abstract Supplement, p. 490, Abs. T11A-13.

Oliver, H.W., and Ponce, D.A., eds., in press in 1994, Major results of geophysical investigations at Yucca Mountain and vicinity, Nevada: U.S. Geological Survey Professional Paper xxxx, ms. 275 p.

Oliver, H.W., Ponce, D.A., and Sikora, R.F., 1991, Major results of gravity and magnetic studies at Yucca Mountain, Nevada: Proceedings of the Second Annual International Conference on High Level Waste Management, Las Vegas, NV, April 28-May 3, 1991, American Nuclear Society, v. 1, p. 787-794.

ref

Oliver, H.W., and Sikora, R.F., 1994, diskette containing gravity and magnetic data across the Ghost Dance Fault in WT-2 Wash, Yucca Mountain, Nevada: U.S. Geological Survey Open-File Report 94-413-B, 4 p., diskette.

delete reference LOCK 9/27

Plouff, Donald, 1977, Preliminary documentation for a FORTRAN program to compute gravity terrain corrections based on topography digitized on a geographic grid: U.S. Geological Survey Open-File Report 77-535, 45 p.

Ponce, D.A., and Oliver, H.W., 1981, Charleston Peak gravity calibration loop, Nevada: U.S. Geological Survey Open-File Report 81-985, 20 p.

Rasmussen, R., and Pedersen, L.B., 1979, End corrections in potential field modeling: Geophysical Prospecting, v. 27, no. 4, p. 749-760.

Rosenbaum, J.G., and Snyder, D.B., 1985, Preliminary interpretation of paleomagnetic and magnetic property data from drill holes USW G1, G2, GU-3, VH-1 and surface localities in the vicinity of Yucca Mountain, Nye County, Nevada: U.S. Geological Survey Open-File Report 85-49, 73 p.

Sawyer, D.A., Fleck, R.J., Lanphere, M.A., Warren, R.G., Broxton, D.E., and Hudson, M.R., in press in 1994, Episodic caldera volcanism in the Miocene southwestern Nevada volcanic field: Revised stratigraphic framework, $^{40}Ar/^{39}Ar$ geochronology, and implications for magmatism and extension: Geological Society of America Bulletin, v. 106, p. xxx.

Smith, Christian, and Ross, H.P., 1982, Interpretation of resistivity and induced polarization profiles with severe topographic effects, Yucca Mountain area, Nevada Test Site, Nevada: U.S. Geological Survey Open-File Report 82-182, 66 p.

Snyder, D.B., and Carr, W.J., 1984, Interpretation of gravity data in a complex volcano-tectonic setting, southwestern Nevada: Journal of Geophysical Research, v. 89, n. B12, p. 10193-10206.

Spengler, R.W., Braun, C.A., Linden, R.M., Martin, L.G., Ross-Brown, D.M., and Blackburn, R.L., 1993, Structural character of the Ghost Dance fault,

Yucca Mountain, Nevada: High Level Radioactive Waste Management, Proceedings of the Fourth Annual International Conference, Las Vegas, Nevada, v. 1, p. 653-659.

Swick, C.A., 1942, Pendulum gravity measurements and isostatic reductions: U.S. Coast and Geodetic Survey Special Publication 232, 82 p.

U.S. Geological Survey, 1984, A summary of geologic studies through January 1, 1983, of the potential high-level radioactive waste repository site at Yucca Mountain, southern Nye County, Nevada: U.S. Geological Survey Open-File Report 84-792, 103 p.

U.S. National Bureau of Standards, 1977, The international system of units (SI): U.S. National Bureau of Standards Special Publication 330, 41 p.

Table 1. Principal facts for gravity stations along profile A-A' (fig. 2). The distances between successive stations are all 150 ft. Abbreviated heading are as follows: "TC A-D 2.67" shows a station listing of inner zone terrain corrections for Hayford zones A-D corresponding to an assumed terrain density of 2.67 g/cm^3; "Total TC 2.67" refers to the total terrain correction for Hayford zones A-O extending to a distance of 103.6 km from each station using a 2.67 g/cm^3 density; "CBA 2.67" is the complete Bouguer anomaly for a 2.67 g/cm^3 assumed density. CBA listings for other assumed densities such as 2.50 g/cm^3, 2.40 g/cm^3, etc., are also shown.

Station No.	Latitude (Deg Min)	Longitude (Deg Min)	Elevation (ft)	Observed gravity (mGal)	Free Air Anomaly (mGal)	Simple Bouguer Anomaly 2.67 mGal	TC A-D 2.67 (mGal)	Total TC 2.67 (mGal)	CBA 2.67 (mGal)	CBA 2.50 (mGal)	CBA 2.40 (mGal)	CBA 2.20 (mGal)	CBA 2.00 (mGal)	CBA 1.80 (mGal)	CBA 1.60 (mGal)
G103	36 49.84	116 27.38	4324.2	979469.13	-14.31	-161.79	111	2.74	-160.37	-151.07	-145.60	-134.66	-123.72	-112.78	-101.84
G102	36 49.85	116 27.36	4309.4	979470.30	-14.55	-161.53	123	2.82	-160.01	-150.75	-145.30	-134.40	-123.51	-112.61	-101.72
G101	36 49.85	116 27.33	4292.9	979471.50	-14.90	-161.31	.89	2.45	-160.17	-150.92	-145.48	-134.60	-123.71	-112.83	-101.95
G1	36 49.87	116 27.28	4268.9	979473.09	-15.59	-161.19	.97	2.49	-160.01	-150.81	-145.40	-134.59	-123.77	-112.95	-102.13
G2	36 49.87	116 27.28	4268.6	979473.33	-15.38	-160.97	.86	2.37	-159.90	-150.70	-145.28	-134.46	-123.63	-112.81	-101.98
G3	36 49.87	116 27.26	4249.4	979474.61	-15.91	-160.84	.94	2.43	-159.71	-150.55	-145.17	-134.40	-123.62	-112.85	-102.08
G4	36 49.88	116 27.33	4233.8	979475.70	-16.30	-160.70	.87	2.38	-159.61	-150.49	-145.12	-134.38	-123.65	-112.91	-102.18
G5	36 49.89	116 27.21	4220.6	979476.56	-16.69	-160.64	.81	2.25	-159.68	-150.58	-145.22	-134.51	-123.80	-113.09	-102.38
G6	36 49.90	116 27.18	4205.8	979477.52	-17.14	-160.58	.93	2.35	-159.52	-150.46	-145.13	-134.46	-123.79	-113.13	-102.46
G7	36 49.91	116 27.15	4193.1	979478.41	-17.46	-160.47	.92	2.32	-159.44	-150.40	-145.08	-134.45	-123.81	-113.18	-102.54
G8	36 49.91	116 27.13	4181.2	979479.40	-17.59	-160.19	.91	2.30	-159.18	-150.17	-144.86	-134.26	-123.65	-113.05	-102.44
G9	36 49.90	116 27.10	4171.6	979480.20	-17.68	-159.95	.81	2.18	-159.06	-150.06	-144.76	-134.17	-123.58	-112.99	-102.40
G10	36 49.90	116 27.07	4155.5	979481.46	-17.93	-159.66	.97	2.32	-158.62	-149.66	-144.39	-133.85	-123.31	-112.78	-102.24
G11	36 49.90	116 27.04	4143.2	979482.49	-18.06	-159.36	.98	2.31	-158.33	-149.40	-144.15	-133.64	-123.13	-112.62	-102.12
G12	36 49.89	116 27.01	4131.0	979483.49	-18.19	-159.08	.89	2.21	-158.15	-149.24	-144.00	-133.51	-123.03	-112.54	-102.06
G13	36 49.88	116 26.99	4119.7	979484.41	-18.32	-158.82	.77	2.08	-158.02	-149.13	-143.89	-133.43	-122.96	-112.50	-102.03
G14	36 49.87	116 26.96	4108.3	979485.24	-18.54	-158.66	.82	2.11	-157.82	-148.95	-143.74	-133.31	-122.87	-112.44	-102.01
G15	36 49.86	116 26.94	4095.6	979486.45	-18.51	-158.20	.59	1.87	-157.60	-148.74	-143.53	-133.11	-122.69	-112.28	-101.86
G16	36 49.85	116 26.91	4082.8	979487.48	-18.67	-157.92	.53	1.80	-157.39	-148.56	-143.36	-132.97	-122.58	-112.19	-101.80
G17	36 49.84	116 26.88	4074.2	979488.20	-18.74	-157.70	.49	1.74	-157.23	-148.41	-143.22	-132.85	-122.48	-112.10	-101.73
G18	36 49.83	116 26.86	4063.5	979489.06	-18.88	-157.47	.44	1.68	-157.05	-148.26	-143.08	-132.73	-122.38	-112.03	-101.68
G19	36 49.83	116 26.83	4052.5	979489.98	-18.99	-157.21	.37	1.60	-156.87	-148.09	-142.93	-132.60	-122.27	-111.94	-101.62
G20	36 49.83	116 26.80	4041.0	979490.69	-19.36	-157.19	.32	1.54	-156.91	-148.15	-143.00	-132.70	-122.40	-112.09	-101.79
G21	36 49.83	116 26.77	4030.0	979491.61	-19.48	-156.92	.25	1.46	-156.73	-147.99	-142.85	-132.57	-122.29	-112.01	-101.72
G22	36 49.83	116 26.74	4020.0	979492.34	-19.69	-156.79	.26	1.46	-156.60	-147.88	-142.75	-132.50	-122.24	-111.98	-101.73
G23	36 49.83	116 26.71	4008.7	979493.23	-19.86	-156.58	.18	1.37	-156.47	-147.77	-142.66	-132.42	-122.19	-111.96	-101.72
G24	36 49.83	116 26.68	3998.8	979494.01	-20.01	-156.39	.19	1.37	-156.28	-147.61	-142.50	-132.29	-122.09	-111.88	-101.67
G25	36 49.83	116 26.68	3988.6	979494.84	-20.14	-156.17	.20	1.39	-156.04	-147.39	-142.30	-132.12	-121.94	-111.76	-101.58
G26	36 49.83	116 26.62	3979.8	979495.57	-20.24	-155.97	.19	1.35	-155.88	-147.24	-142.16	-132.00	-121.84	-111.68	-101.52
G27	36 49.82	116 26.59	3972.4	979495.92	-20.57	-156.05	.13	1.28	-156.02	-147.40	-142.33	-132.18	-122.03	-111.89	-101.74
G28	36 49.82	116 26.56	3964.5	979496.51	-20.72	-155.93	.14	1.28	-155.90	-147.30	-142.23	-132.11	-121.98	-111.85	-101.73

Table 2. Magnetic measurements along profile A-A'. Elevations of the magnetic stations are 8 ft higher than the corresponding gravity stations (Table 1) because the magnetic sensor is at the top of an 8 ft pole. Elevations of intermediate magnetic measurements were linearly interpolated between the surveyed stations G104, G103, G102, etc. and are prefixed by an x.

Station Number	Distance (ft)	Elevation (ft)	Total Magnetic Field (nT)	Station Nubmer	Distance (ft)	Elevation (ft)	Total Magnetic Field (nT)
G104	0	4340	50907	G9100	1900	x4168	51115
G103b	50	x4338	50908	G10	1950	4163	51177
G103a	100	x4335	50899	G1050	2000	x4159	51166
G103	150	4332	50913	G1010	2050	x4155	51150
G102b	200	x4327	50941	G11	2100	4151	51106
G102a	250	x4322	50947	G1150	2150	x4148	51102
G102	300	4317	50953	G1110	2200	x4143	51070
G101b	350	x4311	50950	G12	2250	4139	51088
G101a	400	x4315	50950	G1250	2300	x4135	51084
G101	450	4300	50953	G1210	2350	x4131	51084
G1b	500	x4292	50979	G13	2400	4127	51053
G1a	550	x4284	50994	G1350	2450	x4124	51031
G1	600	4276	50977	G1310	2500	x4120	51019
G1050	650	x4277	51000	G14	2550	4116	50988
G1100	700	x4277	51014	G1450	2600	x4112	50971
G2	750	4276	51013	G1410	2650	x4108	50961
G2050	800	x4270	50977	G15	2700	4103	50959
G2100	850	x4263	51009	G1550	2750	x4098	50929
G3	900	4257	51060	G1510	2800	x4094	50876
G3050	950	x4252	51080	G16	2850	4090	50918
G3100	1000	x4247	51076	G1650	2900	x4088	51002
G4	1050	4241	51116	G1610	2950	x4085	51064
G4021	1071	x4239	51143	G17	3000	4082	51037
G4042	1092	x4236	51179	G1750	3050	x4078	51017
G4063	1113	x4233	51206	G1710	3100	x4075	51047
G4082	1134	x4230	51223	G18	3150	4071	51039
G4103	1155	x4227	51211	G1850	3200	x4068	51017
G4124	1176	x4224	51148	G1810	3250	x4064	51047
G5	1200	4222	50981	G19	3300	4060	50929
G5021	1221	x4221	50841	G1950	3350	x4056	50914
G5042	1242	x4220	50771	G1910	3400	x4052	50909
G5063	1263	x4219	50758	G20	3450	4048	50911
G5084	1284	x4218	50698	G2050	3500	x4045	50930
G5105	1305	x4216	50741	G2010	3550	x4041	50966
G5126	1326	x4215	50811	G21	3600	4038	51007
G6	1350	4213	50651	G2150	3650	x4034	50955
G6017	1367	x4213	50895	G2110	3700	x4031	50882
G6034	1384	x4212	50940	G22	3750	4028	50861
G6051	1401	x4211	50979	G2250	3800	x4024	50869
G6A	1418	4209	51000	G2210	3850	x4020	50894
6A017	1435	x4207	51058	G23	3900	4016	50940
6A034	1452	x4205	51116	G2350	3950	x4012	50975
6A051	1469	x4204	51154	G2310	4000	x4009	51000
6A068	1486	x4202	51168	G24	4050	4006	50991
G7	1500	4201	51135	G2450	4100	x4002	50966
G7020	1520	x4199	51195	G2410	4150	x3999	50974
G7040	1540	x4198	51200	G25	4200	3996	50936
G7060	1560	x4196	51194	G2550	4250	x3993	50901
G7080	1580	x4195	51183	G2510	4300	x3990	50890
G7100	1600	x4193	51169	G26	4350	3987	50905
G7120	1620	x4192	51148	G2650	4400	x3991	50973
G7140	1640	x4190	51127	G2610	4450	x3995	51072
G8	1650	4189	51008	G27	4500	4000	51179
G8050	1700	x4185	51149	G2750	4550	x3990	51195
G8100	1750	x4182	51220	G2710	4600	x3981	51080
G9	1800	4179	51234	G28	4650	3972	51042
G9050	1850	x4173	51184				

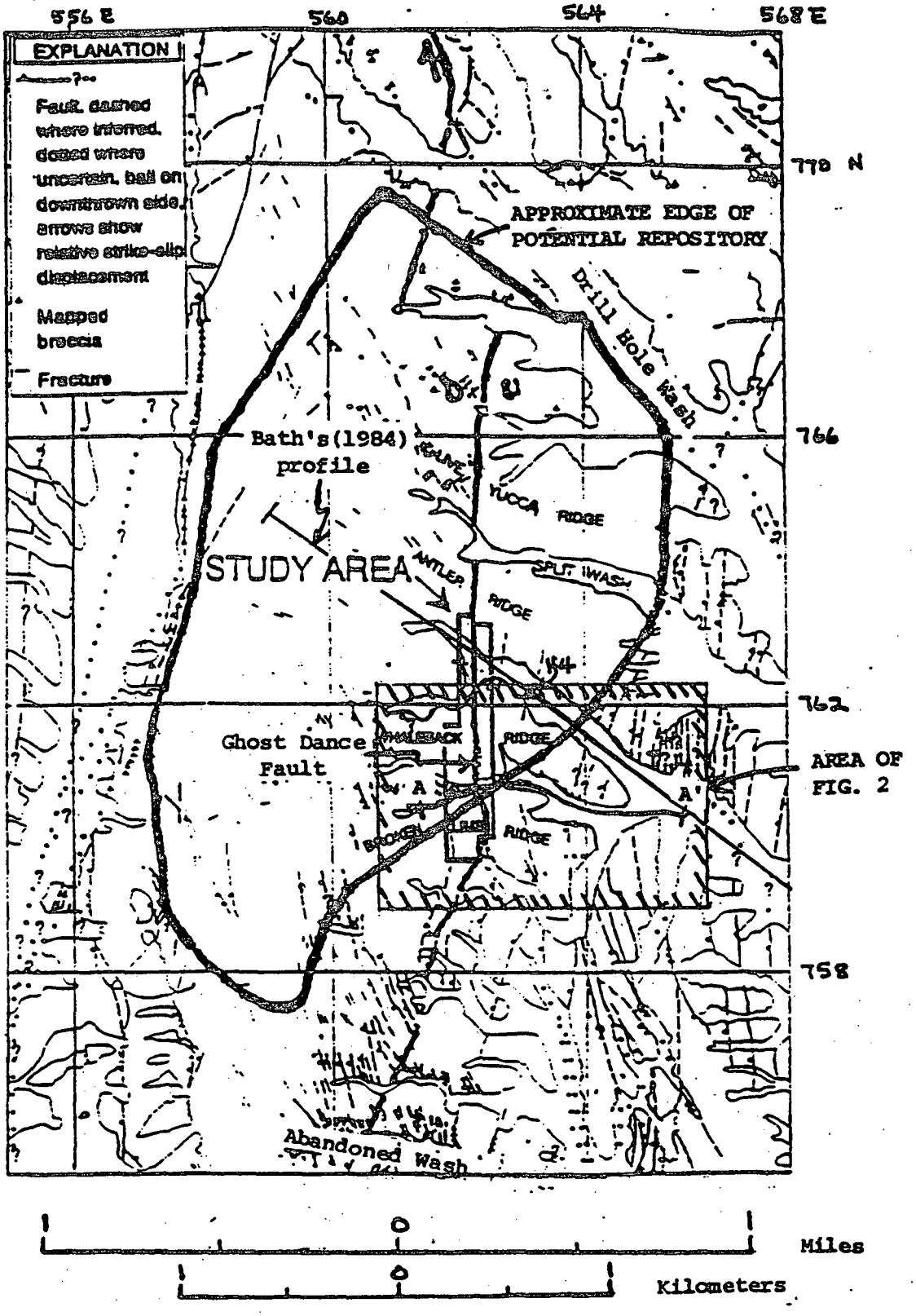

Figure 1. Index map showing new gravity and ground magnetic profile A-A' and its location relative to the potential repository, the Ghost Dance Fault, and geologic "study area" and Bath's(1984)ground magnetic profile through "H4 Wash"north of Whale Back Ridge. Reference lines are Nevada State coordinates in thousands of feet. After Spengler and others(1993,fig.1). Scale 1:27,600.

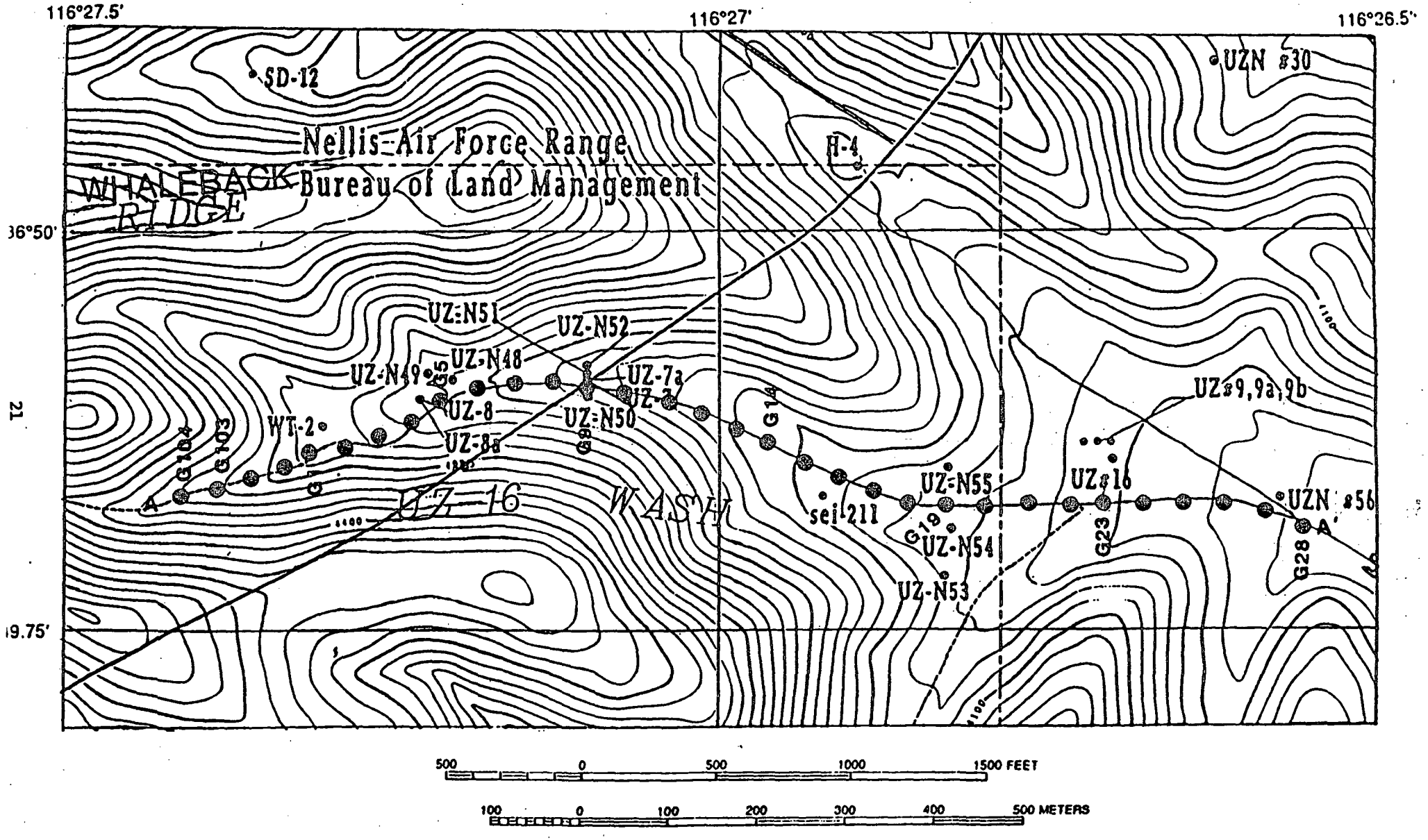

Figure 2. Topographic index map showing location of profile A-A' and all gravity stations. G103 is the westernmost gravity station and the station numbers progress easterly as G102, G101, G1, G2, ...G5, ...G28. All G stations are 150 ft apart (fig. 3). Ground magnetic measurements were also made at all G stations as well as many intermediate points (fig. 4). Scale 1:6,000.

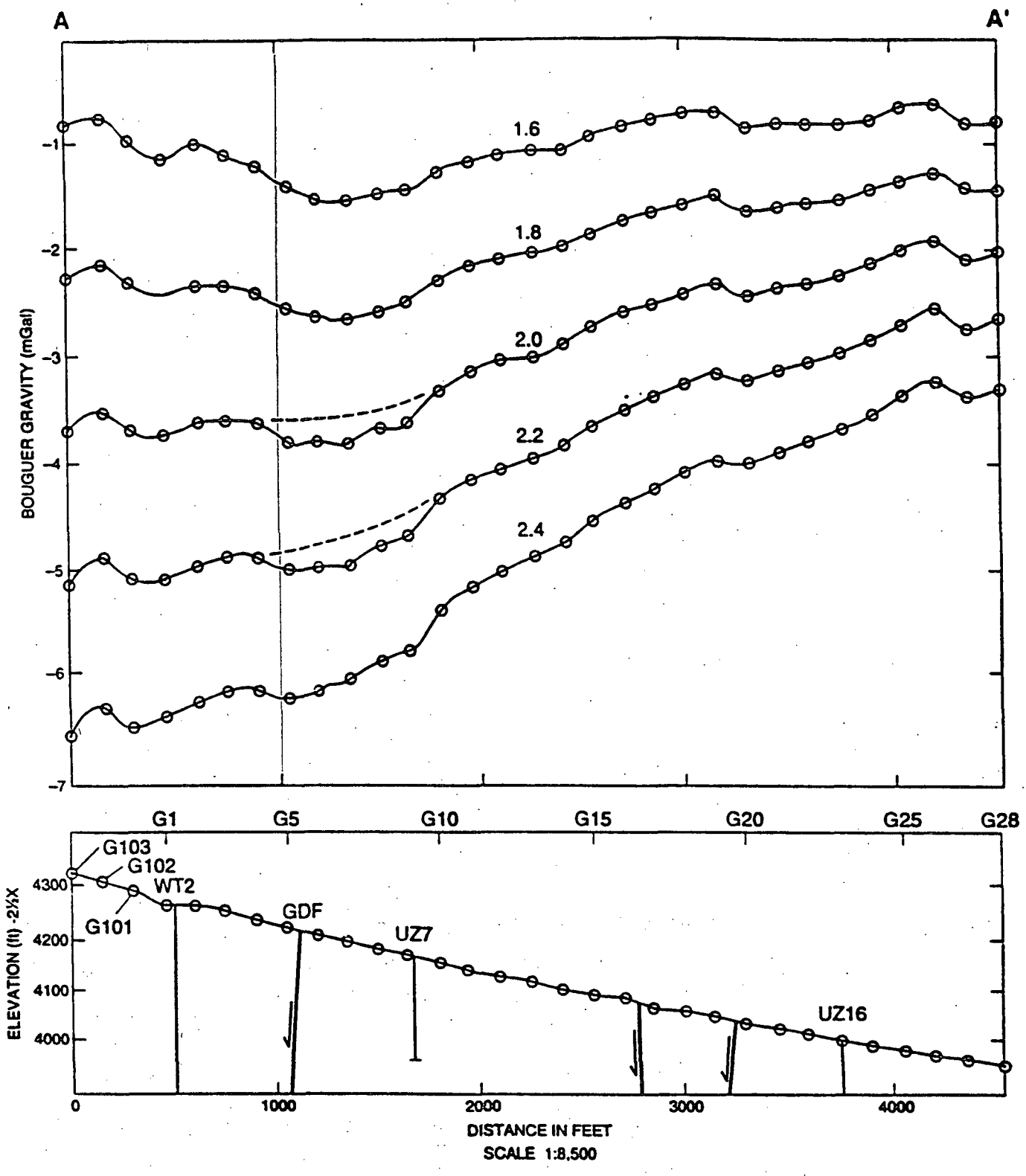

Figure 3. Bouguer gravity profiles along A-A'(fig.2)for reduction densities 1.6,1.8,2.0,2.2,and 2.4 g/cm . The elevation profile shows the location of the Ghost Dance Fault(GDF),two other faults near G16 and G20 based on seismic reflection studies(Majer and Karageorgi, 1994), and drill holes WT-2 and UZ-16. Vertical exaggeration of the elevation profile is 2.5.

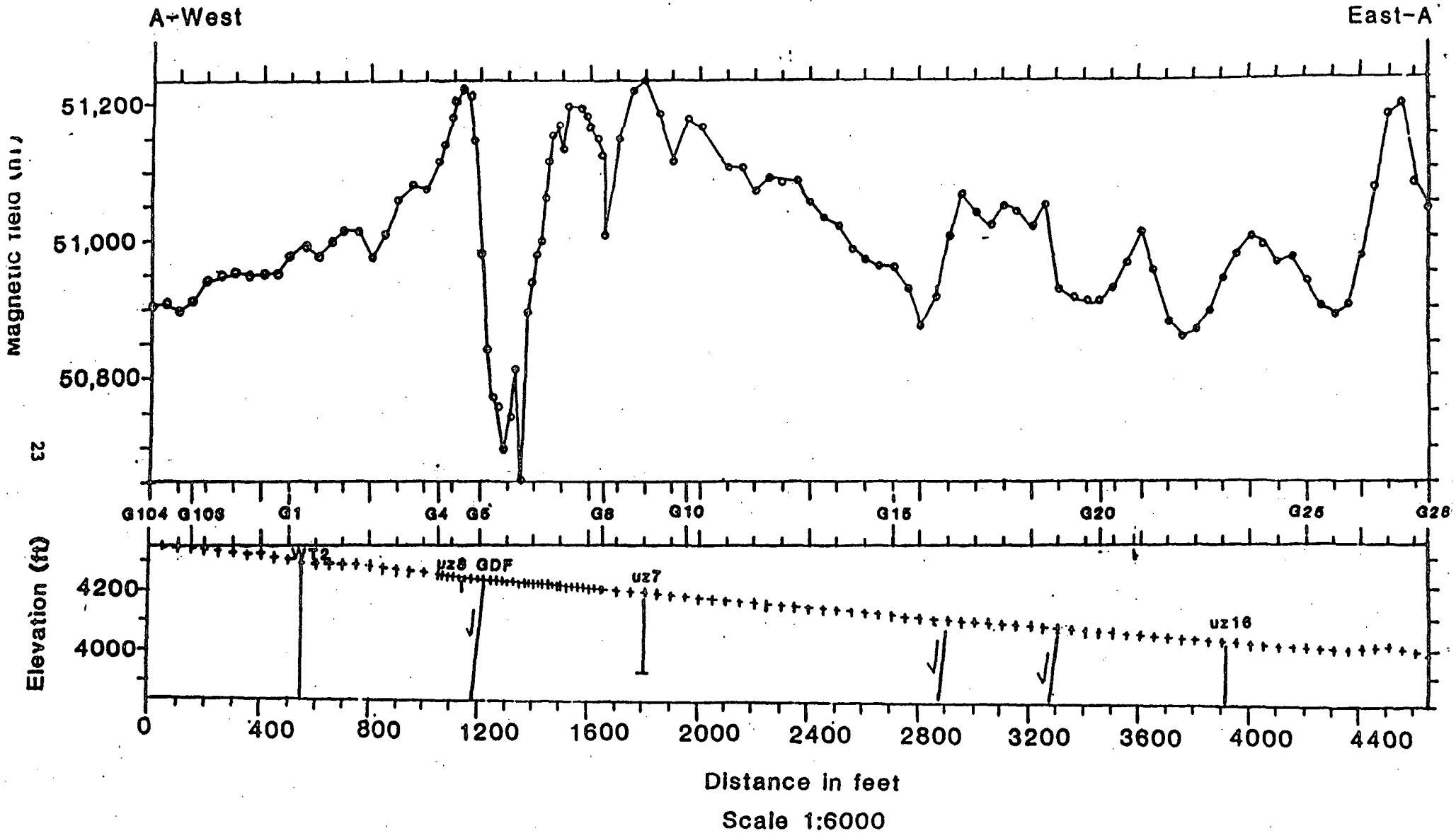

Figure 4. Total magnetic field measurements along profile A-A'(fig. 2). Station spacing of 50 ft for the whole profile was decreased to about 20 ft between G4 and G8. The projected location of the Ghost Dance fault(GDF) within UZ-16 Wash is near station G5. The two faults shown near distanees of 2800 and 3200 ft are based on seismic reflection data(Majer and Karageorgi, 1994). Vertical exaggeration of the elevation profile is 1.1:1.

TIS-950008

United States Department of the Interior

GEOLOGICAL SURVEY
Box 25046 M.S. 425
Denver Federal Center
Denver, Colorado 80225

IN REPLY REFER TO:

I-362670

September 29, 1994

Robert M. Nelson, Jr., Acting Project Manager
Yucca Mountain Site Characterization Project Office
Nevada Field Office
U.S. Department of Energy
P.O. Box 98608

WBS: 1.2.3.2.2.1.1
QA: QA

Attn: Jerry J. Lorenz, REECo, Technical Information Section

SUBJECT: PUBLICATIONS--Transmittal of Report entitled, "Gravity and Magnetic Data across the Ghost Dance Fault in WT-2 Wash, Yucca Mountain, Nevada", by H.W. Oliver and R.F. Sikora

Interagency Agreement No. DE-AI08-92NV10874

Dear Bob:

Two copies of the subject report are enclosed for review in your office and concurrence.

This report received USGS technical review by David Campbell and V. Langenheim who were chosen because of their general knowledge of the work and techniques. A QA review was performed by Martha Mustard, YMPB-QA Office, and a preliminary Policy review was performed by Bob Lewis, YMPB.

Technical data for this report have been submitted in accordance with YAP-SIII.3Q. The tracking number for the TDIF associated with these data is GS940808314212.004

This report was prepared under WBS number 1232211. This is a level-3 milestone - 3GGU440M, with a due date 4/29/94.

Robert E. Lewis, Reports Improvement Officer
Yucca Mountain Project Branch
For: Larry R. Hayes, Chief YMPB

Enclosures
cc w/o enclosures:
LRC File 3.304-9 (P)
L.R. Hayes, YMPB, Denver, CO
J.S. Stuckless, GSP, Denver, CO
B.T. Brady, HIP, YMPB, Denver, CO
T. Mendez-Vigo, USGS/SAIC, Denver, CO
R. Ritchey, YMPB, Denver, CO
YMP WBS Manager: M. Tynan, DOE, NV

DIVISION
cc: LINDENBURG
LORENZ (3)

10/3/94

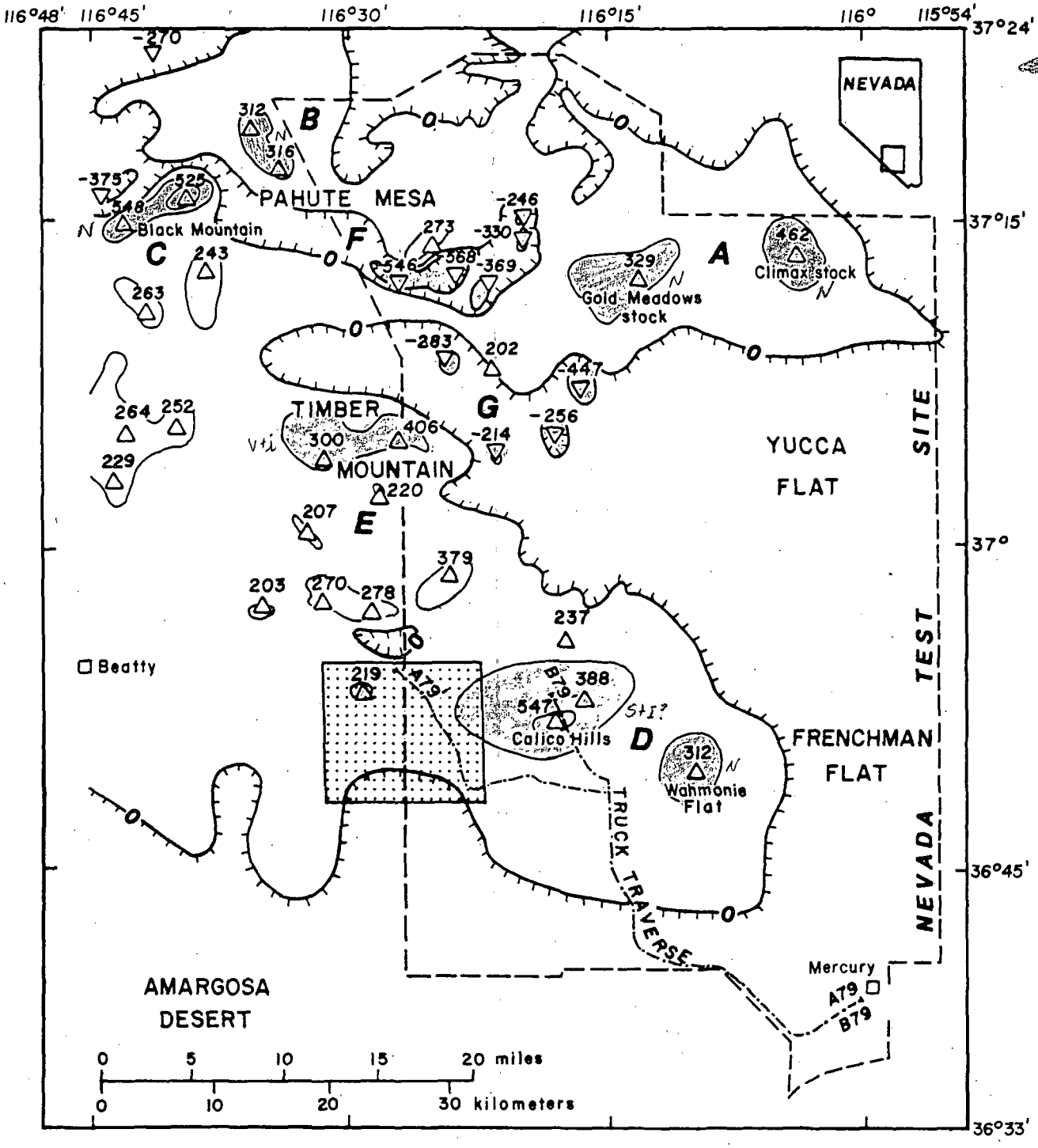

Figure 1.--Residual aeromagnetic map of Nevada Test Site and nearby areas showing the Yucca Mountain area (shaded), areas of outstanding anomaly maxima by letters A through E, and areas of outstanding anomaly minima by letters F and G. Also shown are truck-borne magnetometer traverses A79-A79' and B79-B79' from Mercury to the Yuccca Mountain and Calico Hills areas.

USGS-OFR-91-46

U.S. DEPARTMENT OF THE INTERIOR

GEOLOGICAL SURVEY

Revision of an aeromagnetic survey of the Lathrop Wells area, Nevada[1]

By

V.E. Langenheim, S.F. Carle, D.A. Ponce, and J.D. Phillips

1991

Open-File Report 91-46

Prepared in cooperation with the
Nevada Operations Office
U.S. Department of Energy
(Interagency Agreement DE-AI08-78ET44802)

Menlo Park, California
1991

[1]A magnetic tape of the revised aeromagnetic data of the Lathrop Wells area is available from the National Geophysical Data Center, National Oceanic and Atmospheric Administration, Mail Code E/Gcx2, 325 Broadway, Boulder, CO 80303.

CONTENTS

TABLES

ILLUSTRATIONS

ABSTRACT

Review of an aeromagnetic survey of the Lathrop Wells area revealed two independent problems: (1) regularly spaced intervals of data amounting to one-quarter of the original flightline data are missing and (2) horizontal positioning errors are common. The horizontal positioning errors are as large as 900 m (2,950 ft), far greater than the 50-m (150-ft) positioning uncertainties for similar, nearby surveys. Missing records were restored by using interpolated values from the original contract grids. The positions of the flightlines were corrected by photographic methods of flight path recovery. The uncertainty of the corrected positions of the flightline data is about 150 m (500 ft). A new version of the aeromagnetic map of the Lathrop Wells survey has been prepared using the restored and repositioned data points.

INTRODUCTION

In 1977, an aeromagnetic survey of the Lathrop Wells area (fig. 1) was flown and compiled by Aero Service, Houston, Texas, under contract with the U.S. Geological Survey (U.S. Geological Survey, 1978). Part of the flightline data was used to make an aeromagnetic map of Yucca Mountain and surrounding regions, southwestern Nevada (Kane and Bracken, 1983). Subsequent review of the flightline data used to create the Yucca Mountain map revealed that regularly spaced intervals of missing records occurred and that horizontal positioning errors existed. The missing records caused gridded anomalies to appear distorted, and positioning errors caused displacements of gridded anomalies. The horizontal positioning of the Lathrop Wells aeromagnetic survey is important for locating magnetic anomalies associated with volcanic rocks buried by or intruded into alluvial deposits in the Lathrop Wells area.

The characterization of these magnetic anomalies is of interest for determining the rate of volcanism in the Yucca Mountain area, which includes a potential site for a nuclear waste repository.

ACKNOWLEDGMENTS

B.A. Chuchel, J.M. Glen, H.W. Oliver, and K.S. Kirchoff-Stein of the U.S. Geological Survey assisted in planning, analysis, and manuscript review.

The following number is for U.S. Department of Energy OCRWM records management purposes only and should not be used when ordering this publication. Accession number: NNA.910411.0079.

FLIGHTLINE DATA GAPS

The aeromagnetic survey of the Lathrop Wells area, hereafter referred to as the Lathrop Wells survey (LWS), was flown at a 400- and 800-m ($\frac{1}{4}$- and $\frac{1}{2}$-mi) flightline spacing (fig. 2). The northwest "panhandle" of the LWS was flown along north-south flightlines flown at 300 m (1,000 ft) above ground level with 150-m (500-ft) spacing between measurements. The remainder of the LWS, hereafter referred to as the southern portion of the LWS, was covered by east-west flightlines flown at about 120 m (400 ft) above ground level with about 45-m (150-ft) spacing between measurements.

The published aeromagnetic map of the LWS (U.S. Geological Survey, 1978) was made from the original contract flightline data. Hereafter, *original data* refers to the Lathrop Wells aeromagnetic data that contain no gaps and that were used to generate the 1978 aeromagnetic map (U.S. Geological Survey, 1978). Later, an aeromagnetic compilation of Yucca Mountain and surrounding regions (Kane and Bracken, 1983) used data from both the northern and southern portions of the LWS (fig. 1) provided by Aero Service. A comparison of a part of

the Yucca Mountain and surrounding regions map (fig. 2a) with the Lathrop Wells contract map (fig. 2b) shows that anomalies are dropped out or smoothed on the Yucca Mountain map where gaps in data occur. Apparently, data containing gaps, not the original data, were used by Kane and Bracken (1983) for the area covered by the LWS. Hereafter, *data with gaps* refers to the Lathrop Wells aeromagnetic data set provided by Aero Service to the USGS. These gaps were created sometime between 1978 and 1983, perhaps in copying the data from magnetic tapes given by the contractor. The *data with gaps* contain a regular pattern of gaps about 1.2-km ($\frac{3}{4}$-mi) long and spaced 3.6-km ($2\frac{1}{4}$-mi) apart (fig. 3). Review of the *data with gaps* reveals that the gaps are a result of a consistent pattern of 25 missing records followed by 75 intact records for the southern portion of the LWS; the northern panhandle of the LWS consists of a pattern of 25 intact records and eight missing records.

RESTORING THE GAPS

It was determined (D.A. Ponce, B.A. Chuchel, and J.M. Glen, oral commun., 1987) that the original flightline data might be recoverable, but that it would be more cost-effective and less time-consuming to restore the gaps using the contract gridded data generated by Aero Service from the original flightline data. The gaps were restored in two steps. Within each gap, the positions of the missing records were located by linear interpolation between the flightline records that preceded and followed the gap. The linearly interpolated position is equivalent to assuming that within the gap the airplane flew along a straight line with constant velocity. This is a good approximation considering that the length of the gaps is equal to or less than 1.3-km ($\frac{3}{4}$-mi) and that standard photographic methods of flight path recovery often utilize intervals between tie points of greater than 1.3 km. The number of missing records within each gap for the southern part of the LWS was usually 26, implying 25 missing data points. Gaps that terminate at the end of a flightline have less than 25 missing records. For the northern panhandle of the LWS, the number of missing points within a gap

was eight. Gaps that terminated at the end of a flightline in the north-south portion of the LWS have less than eight missing records.

The second step estimated values of the residual magnetic field for each missing record. At each position an anomaly value was interpolated from the contract grid data. However, the contract grid data also contain missing records and erroneous zero values. These missing records and erroneous zero values were replaced with values determined by interpolation from the surrounding grid values. Then, for each missing point along the flightline, an anomaly value was interpolated from the corrected contract grid data. The grid data tend to alias the original flightline data because the spacing between measurements for the LWS is the same or less than the grid cell dimensions; a comparison of the restored map (fig. 4a) with the contract map (U.S. Geological Survey, 1978; fig. 4b) shows that the interpolated anomaly values successfully reproduce the contract map. This is not surprising because the contract map was made from the contract grids.

HORIZONTAL POSITIONING ERRORS

Three independent lines of evidence indicate that the positions of original data points in the southern portion of the LWS, as received from Aero Service, are shifted to the west of their true positions. First, Lathrop Wells survey data are shifted to the west with respect to ground magnetic profiles collected in the vicinity of Lathrop Wells (D.A. Ponce and others, unpub. data, 1986). This was discovered by reduction of ground magnetic data and upward continuation to the same level of the Lathrop Wells survey by K.S. Kirchoff-Stein (written commun., 1986). Here, anomalies in the Lathrop Wells aeromagnetic survey are shifted 250±60 m (820±200 ft) to the west of the corresponding anomalies in the ground magnetic profiles.

Secondly, K.S. Kirchoff-Stein (written commun., 1986) and author J. Phillips independently discovered that the southern portion of the LWS is shifted with respect to an aero-

magnetic survey of the Timber Mountain area (hereafter referred to as the Timber Mountain survey; U.S. Geological Survey, 1979) where they overlap (fig. 1). Grids of the Lathrop Wells data and the Timber Mountain data were compared. Anomalies were uniformly offset by about 300 m (980 ft) in an east-west direction. Anomalies in the Lathrop Wells data were located further to the west than the corresponding anomalies in the Timber Mountain data. The Timber Mountain data include radar and barometric altimetry. These components were gridded and compared to digital terrain data in order to establish that the horizontal positions within the Timber Mountain data set are accurate to within 50 m (160 ft). Consequently, the apparent 300-m (980-ft) westward shift of the Lathrop Wells data with respect to the Timber Mountain data is entirely due to positioning errors of the Lathrop Wells survey. A nearly perfect match of the positions of the anomalies was achieved in the area of overlap by shifting the Lathrop Wells data 300 m (980 ft) to the east.

Thirdly, a comparison with an aeromagnetic survey of the Yucca Mountain area, hereafter referred to as the Yucca Mountain survey (U.S. Geological Survey, 1984; fig. 1), also shows that the LWS is shifted to the west. The Yucca Mountain survey was flown along north-south flightlines, with a 400-m ($\frac{1}{4}$-mi) spacing, and at a constant terrain clearance of 120-m (400-ft).

The area of comparison of the Lathrop Wells survey with the ground magnetic data only amounts to a few square kilometers, overlap with the Timber Mountain survey constitutes only a narrow strip of about 140 km^2, and overlap with the Yucca Mountain survey amounts to about 30 km^2. Therefore, questions remained as to whether or not the positioning errors occur throughout the LWS, have a north-south dependency, a systematic dependency on location, or are related to each flightline independently.

To examine the character of the positioning errors throughout the area of the southern portion of the LWS, barometric altimetry minus radar altimetry of all flightlines and tie-lines were compared with 1:24,000-scale U.S. Geological Survey topographic maps. If the location and altimetry measurements along the flightline are correct, topographic elevations should

be equal to the barometrically-determined elevation of the airplane minus the radar-obtained altitude above terrain. Barometric and radar altimetry were not available for the northern panhandle of the LWS. In localities characterized by distinctive topography, such as north-south trending ridges, the positions of the flightlines were clearly and consistently shifted to the west (fig. 5). However, the magnitude of these recognized shifts (364 in all) varied from 0 to 650 m (2,130 ft), implying that the positioning errors were variable. In addition, some north-south shifts were recognized, implying a north-south variation. Therefore, comparison of the barometric minus radar altimetry with topography revealed that the shift was variable in both east-west and north-south directions, and that a better method was needed to reposition the flightlines in the southern portion of the LWS.

Photographic filmstrip negatives of the ground surface directly beneath the plane were available from Aero Service for every 3 to 10 fiducial numbers along the flightlines and tielines of the northern portion of the LWS, but not for the panhandle. Film records of this sort are normally used to locate positions of selected points along each flightline on topographic quadrangles or to airphotos registered to geographic coordinates (Dobrin, 1976). We chose to verify the positioning by using orthophoto quadrangles because they have been registered to geographic coordinates, whereas the airphotos have not. The resolution of the orthophoto quadrangles, however, is inferior to that of many other unpositioned airphotos.

First, filmstrip negatives were matched with their correct position on the orthophoto quadrangles. Most often, this was possible where features such as roads, stream channels, vegetation, or buildings were readily identifiable on both the filmstrip negatives and the orthophoto quadrangles. This initial examination demonstrated that the positioning errors of the flightlines in the southern portion of the LWS were variable in both an east-west direction and a north-south direction by similar amounts. Generally, shifts are oriented southwest to northeast, from uncorrected to corrected horizontal position, by 0 to 900 m (2,950 ft). Regional trends are apparent in the positioning errors, but some flightlines transgress these regional trends.

As a result of this initial comparison, it was determined that each flightline in the LWS should be adjusted individually rather than shifting the entire survey by a constant amount. To accomplish this, additional comparisons of the filmstrip negatives with the orthophoto quadrangles were made so that at least one, but preferably more than one control point was identified for each flightline. A total of 823 control points were identified for the 88 east-west flightlines (fig. 6). The control points were used for repositioning each flightline. The repositioning was accomplished by a linear correction. Given a flightline with a number of identified positioning errors, $i = 1, n$, where (x_i, y_i) and (x'_i, y'_i) are the original and corrected positions of the control points, then the original position, (x, y), of each data point was adjusted to a new position, (x', y') by:

$$x' = x'_i + \left(\frac{(x - x_i)(x'_{i+1} - x'_i)}{(x_{i+1} - x_i)} \right)$$

$$y' = y + y'_i - y_i + \left(\frac{(x - x_i)(y'_{i+1} - y_{i+1} - y'_1 + y_1)}{x_{i+1} - x_i} \right)$$

where x lies between x_i and x_{i+1}. Where the fiducial number of (x, y) is less than the fiducial number of (x_1, y_1), the shift is a constant based on the first measured shift for that flightline

$$x' = x + x'_1 - x_1$$

$$y' = y + y'_1 - y_1$$

and where the fiducial number of (x, y) is greater than the fiducial number of (x_n, y_n), the shift is again a constant based on the last measured shift for the flightline

$$x' = x + x'_n - x_n$$

$$y' = y + y'_n - y_n$$

The average magnitude of the identified positioning errors is 396 ± 215 m (1300 ± 710 ft). The average magnitude of east-west shifts is nearly the same as that of the north-south shifts (278 ± 184 m (910 ± 605 ft) and 220 ± 209 m (720 ± 690 ft), respectively. The uncertainty in the repositioning of the flightlines is related to the number of identified positioning errors.

Obviously, the more identified control points per flightline, the more accurate the linear interpolation. Another source of uncertainty results from non-linearities in the x-velocity of the airplane. These errors become more pronounced as the flightline direction deviates from the direction of the x-axis. In order to assess the accuracy of the new positions of the flightline data, profiles of barometric altimetry minus radar altimetry were compared with 1:24,000 topographic maps. This comparison showed that the uncertainty in position of the corrected flightline data is about 150 m (500 ft).

CONCLUSIONS

Regularly spaced gaps in the LWS flightline data were restored with values interpolated from the contract gridded data. Maps made from the restored flightline data closely duplicate the original contract map (U.S. Geological Survey, 1978).

The positions of the flightline data of the southern portion of the LWS as received from Aero Service appear to be shifted by variable amounts. Along each flightline, positions were corrected by interpolating the amount of shift determined by comparing the photographic filmstrips of the ground directly beneath the plane with orthophoto quadrangles. Although photographic filmstrips of the northern portion of the LWS were not available, a comparison of the anomalies of the northern portion of the LWS with those of the Timber Mountain survey does not indicate that the LWS flightlines are significantly shifted.

DESCRIPTION OF MAGNETIC TAPE

A nine-track, 1600 bits per inch, 80 character record size, 4,000 character block size, Ascii unlabeled magnetic tape contains the original, restored, and repositioned files (table 1). The magnetic tape is available from the National Geophysical Data Center, National Oceanic and Atmospheric Administration, Mail Code E/Gcx2, 325 Broadway, Boulder, CO 80303. The format of the data files is described in table 2. The tape also contains a file that describes the contents of the other files (readme.txt).

TABLE 1.–*Description of data files on tape*
[LWS, Lathrop Wells survey]

File number	Name	Description
1	README.TXT	Description of tape contents.
		ORIGINAL CONTRACT DATA
2	LWEW.ORIG	Flightline data (with gaps) including tie-line data of the northern portion of the LWS.
3	LWNS.ORIG	Flightline data (with gaps) of the southern portion of the LWS; tie-line data not available.
4	LWNS1.GRD	Contract grid data for sheet 1 of U.S. Geological Survey (1978).
5	LWEW2.GRD	Contract grid data for sheet 2 of U.S. Geological Survey (1978).
6	LWEW3.GRD	Contract grid data for sheet 3 of U.S. Geological Survey (1978).
		RESTORED DATA FILES
7	LWEW.RES	Flightline data of the east-west portion of the LWS, with zero values deleted, and gaps filled by contract grid data.
8	LWNS.RES	Flightline data of the north-south portion of the LWS, with zero values deleted and gaps filled by contract grid data.
9	LWEWTIE.RES	Tieline data of the east-west portion of the LWS, with gaps filled by contract grid data.
		RESTORED AND REPOSITIONED DATA FILE
10	LWEW.REP	Flightline data of restored east-west portion of LWS, repositioned by comparison of orthophoto quadrangles and filmstrip negatives.

TABLE 2.–*Format of data files on tape*
[IGRF, International Geomagnetic Reference Field]

Format	Description
	FIRST TEN RECORDS OF EACH FILE
Record:	
1	File type (1=gridded, 7=ASCII) and creation date.
2	File name.
3	Description of file contents.
4	FORTRAN format of each record.
5	Information on file format.
6	Information on grid data, if applicable.
7	More information on grid data, if applicable.
8	Descriptive text.
9	Descriptive text.
10	Descriptive text.
	FLIGHTLINE DATA FILE
Beginning at record 11. ten items per record, Item:	
1	Flightline identification.
2	Flightline identification.
3	Longitude, in decimal degrees.
4	Latitude, in decimal degrees.
5	Total field minus IGRF, in nanoteslas.
6	Total field, in nanoteslas.
7	Height above terrain, in meters.
8	Barometric altitude, in meters.
9	Fiducial number.
10	Year and day, yr.day
	GRID DATA FILE
Beginning at record 11 four items per record, Item:	
1	Latitude of center of grid cell, in decimal degrees.
2	Longitude of center of grid cell, in decimal degrees.
3	Total field minus IGRF, in nanoteslas.
4	Total field, in nanoteslas.

REFERENCES

Dobrin, M.B., 1976, Introduction to Geophysical Prospecting: New York, McGraw-Hill Book Co., 630 p. NNA.890713.0200.

Kane, M. F. and Bracken, R. E., 1983, Aeromagnetic map of Yucca Mountain and surrounding regions, southwest Nevada: U.S. Geological Survey Open-File Report 83-616, 19 p, scale 1:48,000. HQS.880517.1290.

U.S. Geological Survey, 1978, Aeromagnetic map of the Lathrop Wells area, Nevada: U.S. Geological Survey Open-File Report 78-1103, scale 1:62,500, 3 sheets. NNA. 901005.0050.

U.S. Geological Survey, 1979, Aeromagnetic map of the Timber Mountain area, Nevada: U.S. Geological Survey Open-File Report 79-587, scale 1:62,500, 3 sheets. NNA.910220. 0059.

U.S. Geological Survey, 1984, Aeromagnetic map of the Yucca Mountain area, Nevada: U.S. Geological Survey Open-File Report 84-206, scale 1:62,500. NNA.910306.0173.

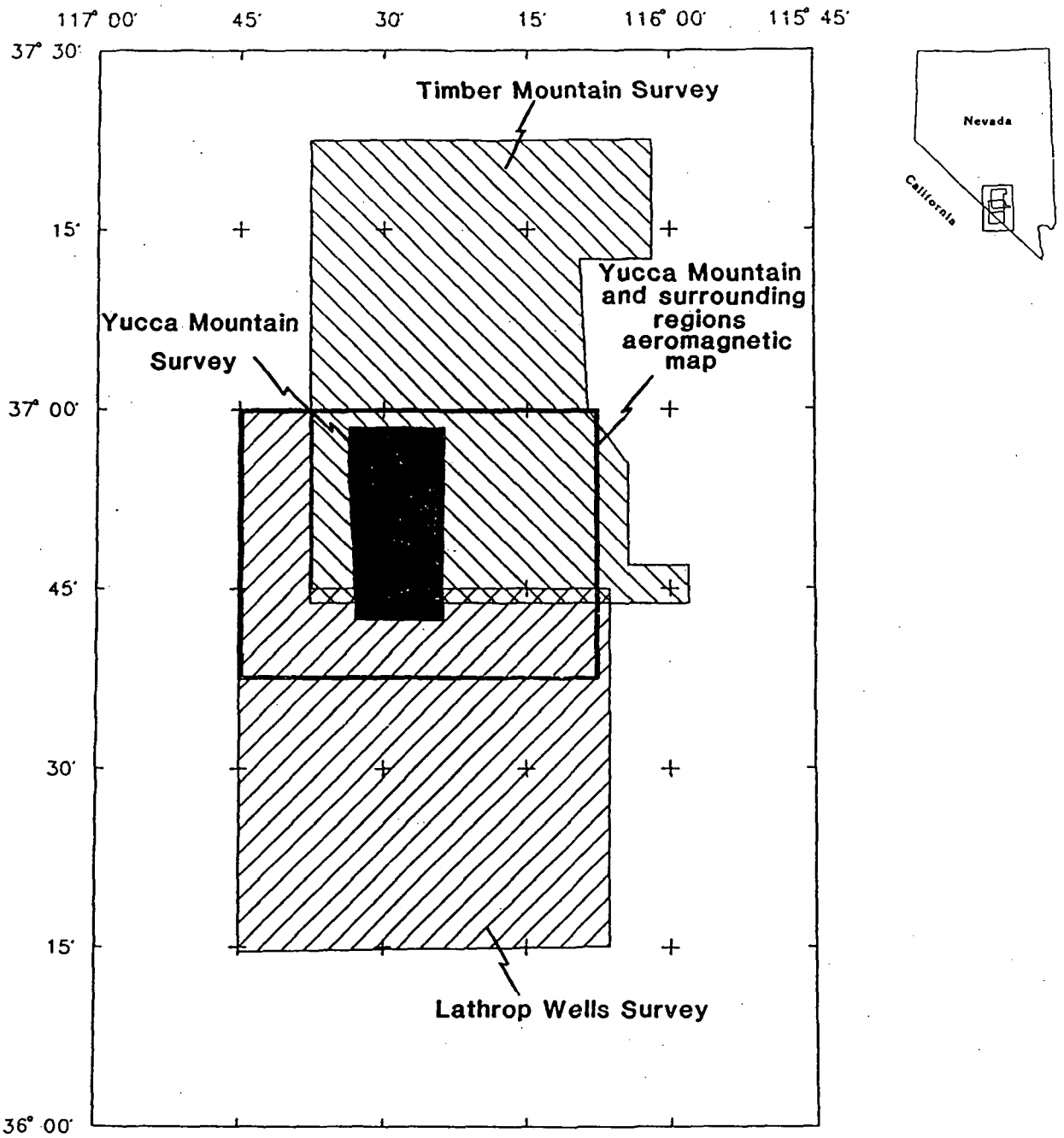

FIGURE 1.–Index map showing the locations of the Lathrop Wells, Timber Mountain, and Yucca Mountain aeromagnetic surveys. Bold outline indicates boundary of the Yucca Mountain and surrounding region aeromagnetic map (Kane and Bracken, 1983), a compilation of the Lathrop Wells and Timber Mountain surveys..

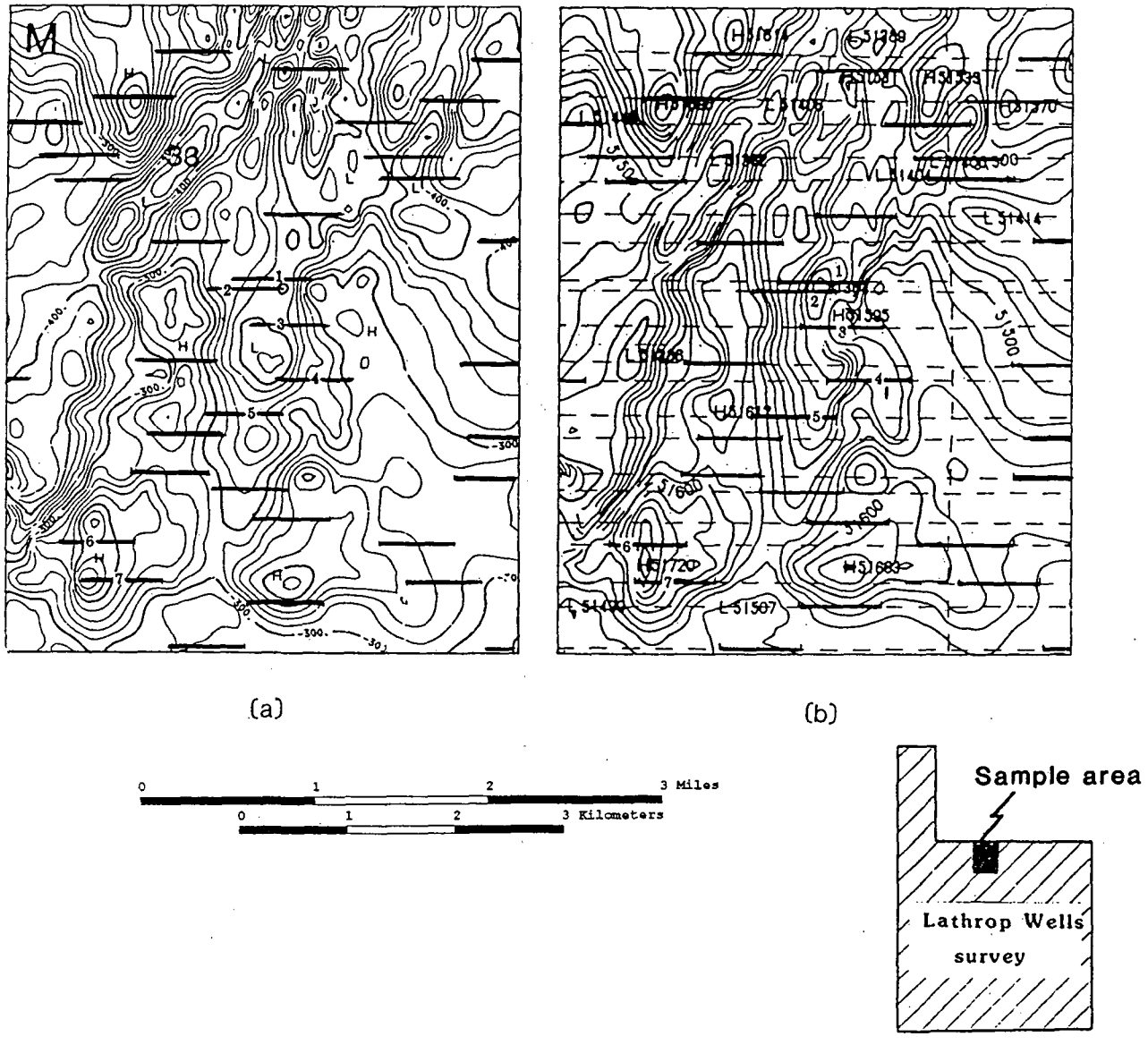

FIGURE 2.–Comparison of (a) Kane and Bracken (1983) map and (b) U.S. Geological Survey (1978) map in sample area. Noticeable discrepancies between these two maps occur in the flightline data gaps, as exemplified by gaps labeled 1-7. Bold lines, flightline data gaps.

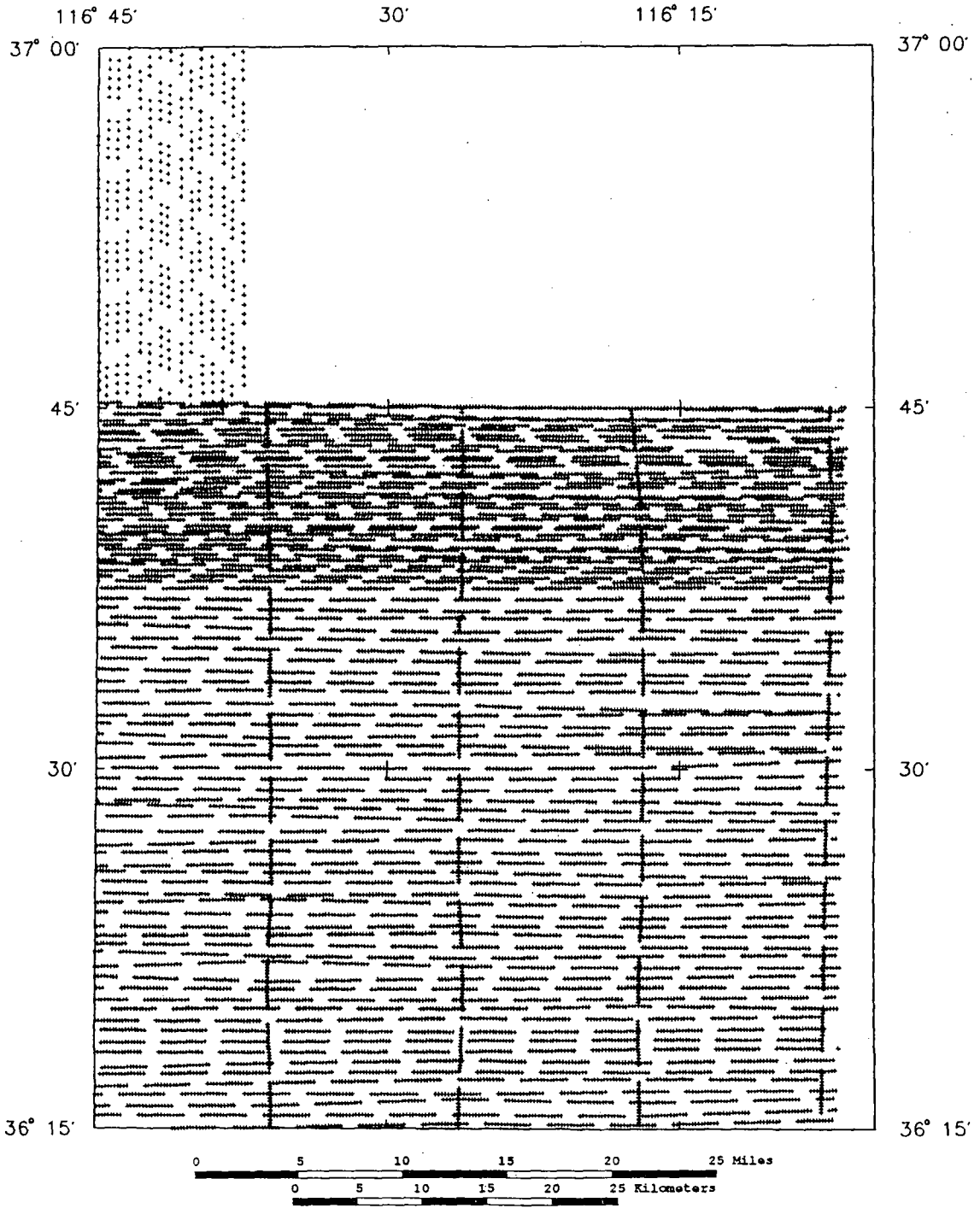

FIGURE 3.–Flightline locations of the Lathrop Wells survey as supplied by Aero Service showing the location of every fifth data point and gaps caused by missing data records.

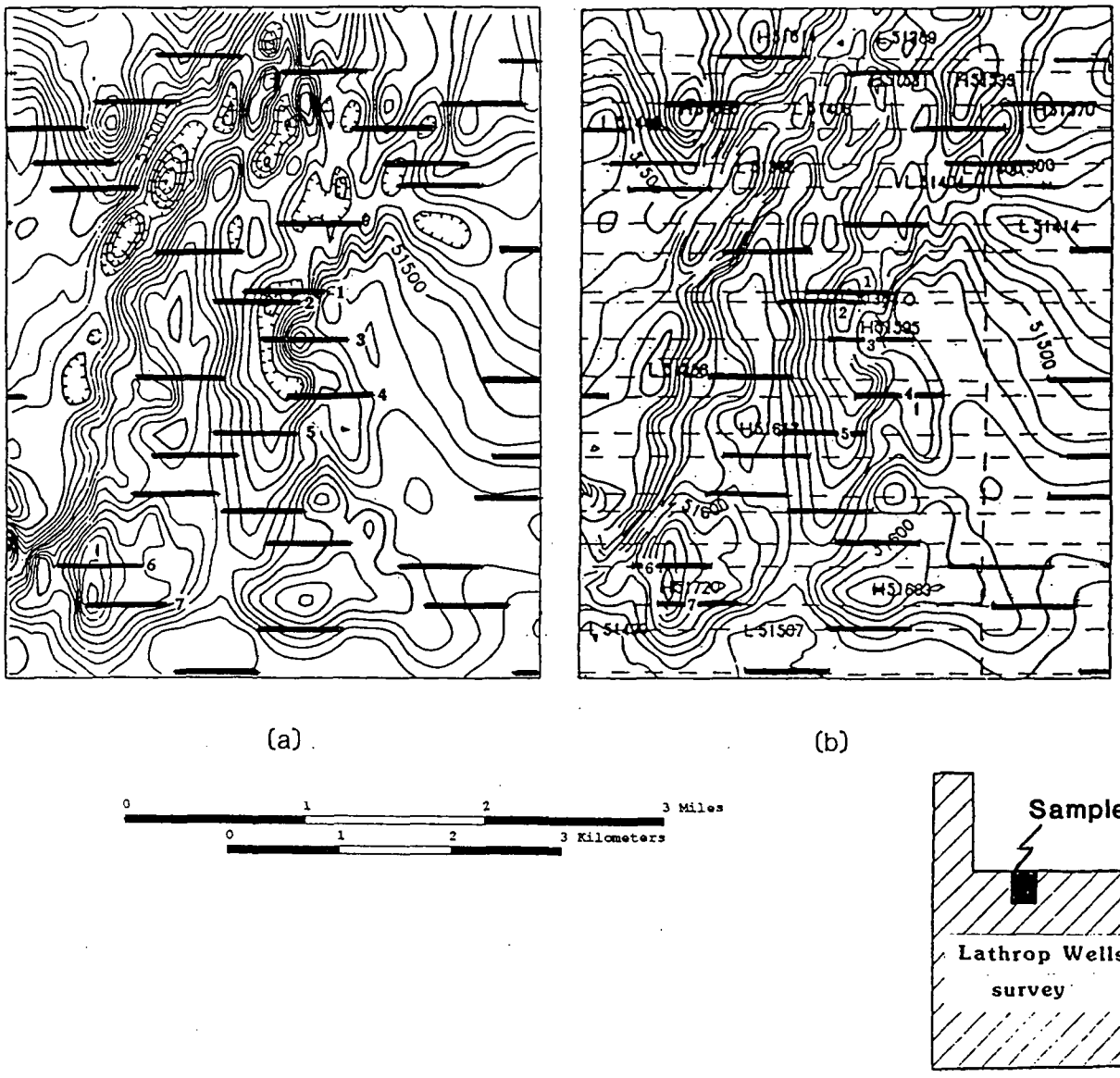

FIGURE 4.–Comparison of the (a) restored map with the (b) U.S. Geological Survey (1978) map. Note that the portions of the restored map controlled by the gridded data (bold lines) closely match the portions of the U.S. Geological Survey (1978) map controlled by original flightline data.

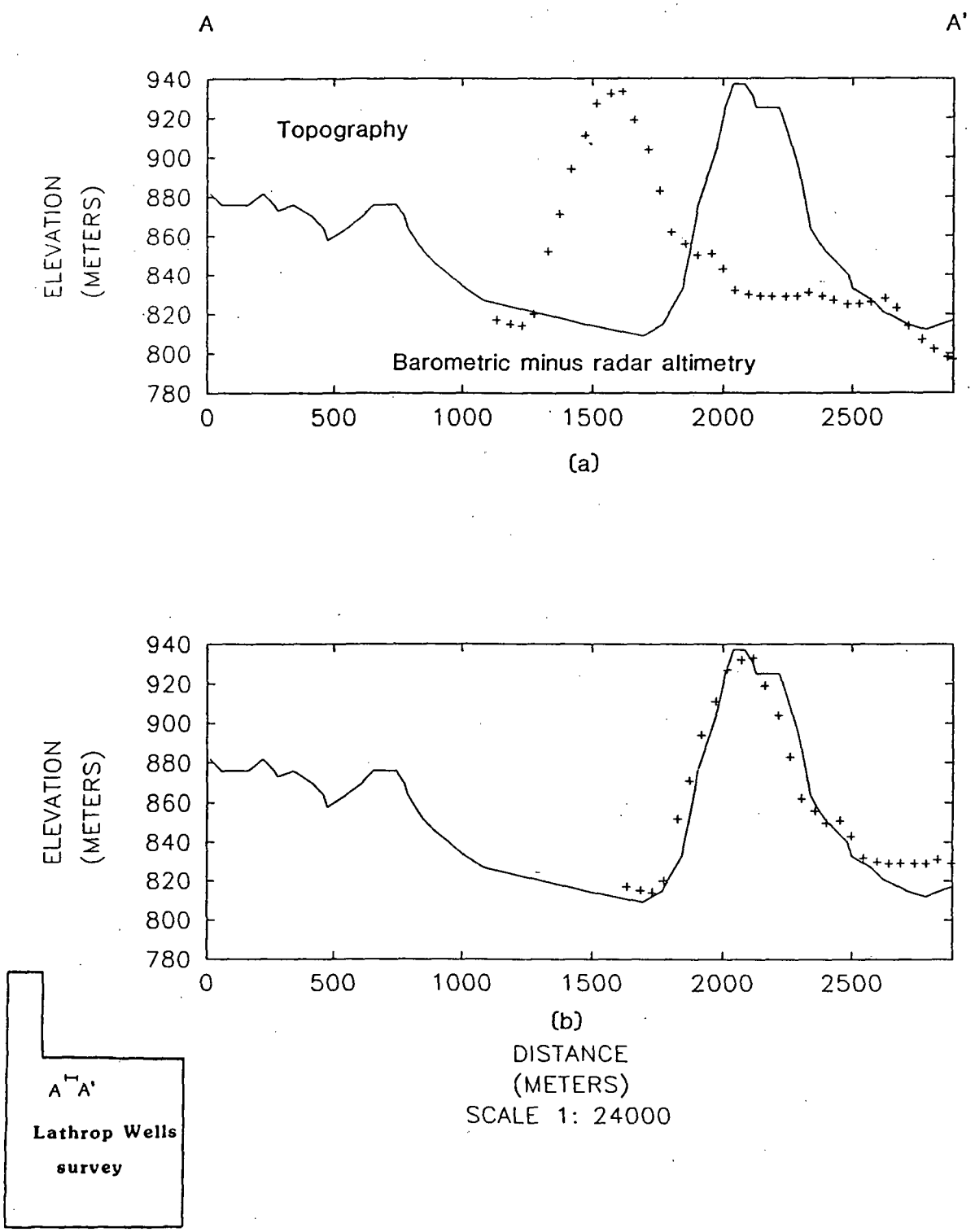

FIGURE 5.–Comparison of corrected positions (a) and uncorrected positions (b) determined by analysis of barometric minus radar altimetry and topography digitized from a 1:24,000-scale topographic map. The position of the LWS flightline was shifted about 500 m (1,640 ft) to the east in order to correct the error in location.

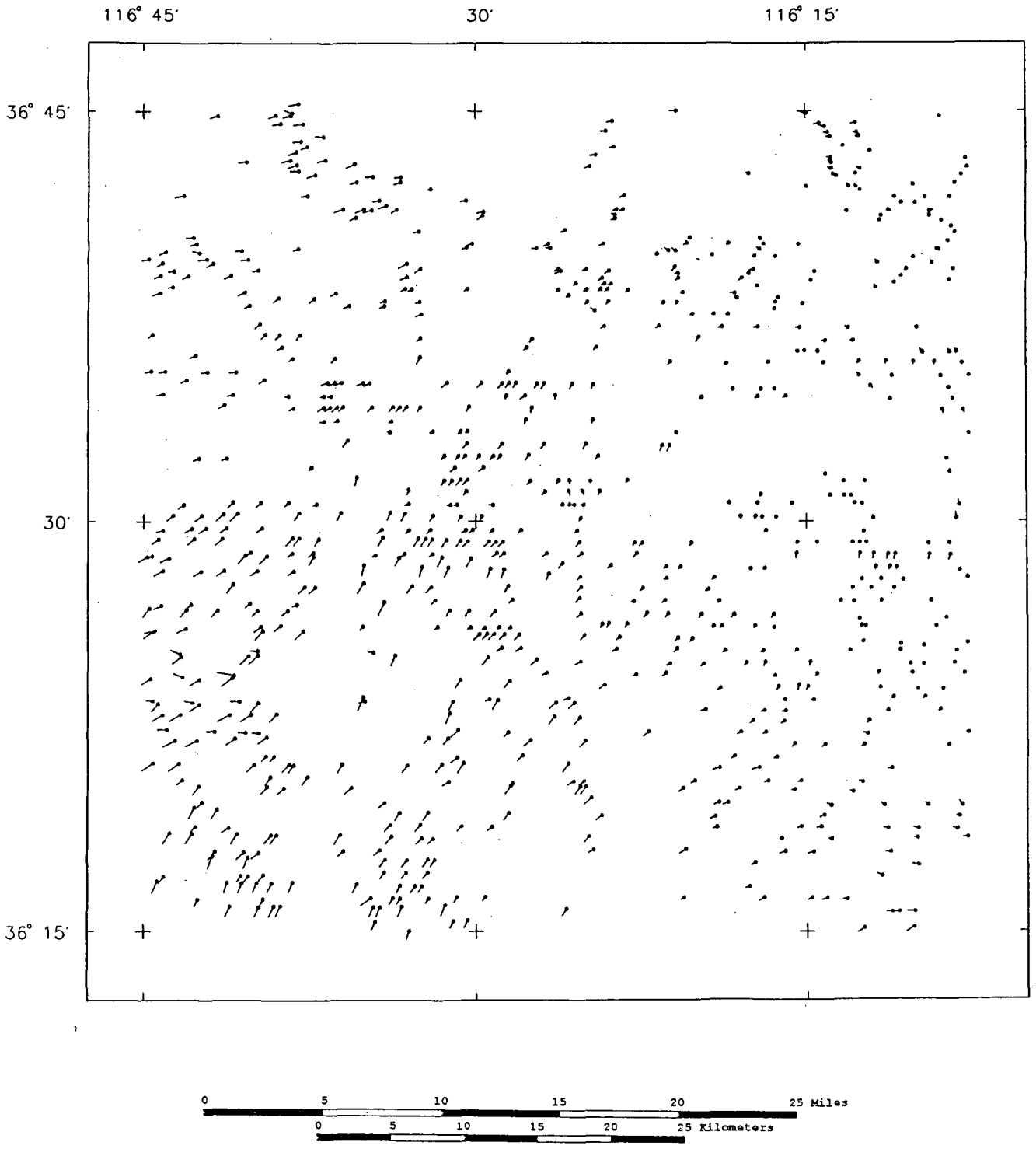

FIGURE 6.–Directions and magnitudes of corrections to the positioning of the east-west portion of the Lathrop Wells survey. Corrections were determined by comparison of the filmstrip negatives and orthophoto quadrangles and vary from 0 - 900 m (0 - 2,950 ft). Dashes denote direction and magnitude of corrections; length of dash is proportional to magnitude of correction. Circles indicate corrected locations. Diameter of circles is 200 m (660 ft) at scale of figure.

☆ U.S. GOVERNMENT PRINTING OFFICE: 1991—587-681

Yucca Mtn, NV

Yucca Mtn, NV 116°35' W long
36°50' N lat

	1975	1980
Total Field Int	51,800 (-35 nT/y)	51,625 ext.
Decl.	14.5 E ex 5.0	14.95° E
Incl. (	62° N (-1.0'/yr)	62° N

$0.51800 \times 10^{-4} T \times 10^{4}$ gauss/T

$T = 51{,}700\ {}^{\gamma}nT = 51{,}700 \times 10^{-9} T = 0.51700 \times 10^{-4} T = 0.51700$ gauss

Variation: +5.64 nT/km N
+1.72 nT/km E

B & J = Tesla
M & H = A/m

J & M = emu/cc
B gauss
H oersted

	SI	cgs
SI	$B = \mu_0 H + J$	$B = H + 4\pi J$
	$J = \mu_0 M$	$J = M$
	$\mu_0 = 4\pi \times 10^{-7}$ H/m	
	$M = J/\mu_0 = kH$	$M = J = kH$
	4π SI $\Leftarrow$	1 cgs

1 Tesla = 10^4 gauss

cgs	S.I.
$M = J = kH$	$M = J/\mu_0 = kH$
	$M = kH$
	$= (k \quad)(.517 \times 10^{-4}\ T)$
	Defn.
	$M = \frac{J}{\mu_0} = \frac{1\ T}{4\pi \times 10^{-7}}$
	$= \frac{10^7}{12.566} \times 10^5 = 7.9575$
$k = \frac{J}{H} =$	$k = \frac{M}{H} = \frac{M(A/m)}{.517 \times 10^{-4}\ T}$

SI $1\ A/m = kH = 4\pi \times 10^{-3}\ Oe = [k \quad] \times 12.57\ [0.5\ Oe]\ [10^{-3}]$

cgs $1\ A/m = 10^{-3}\ emu/cm^3 = [2,000 \times 10^{-6}\ cgs]\ [0.5\ Oe]$
$= 1,000 \times 10^{-6} = 10^{-3}\ emu/cm^3$

See Bath, G.D. et al, 1983, Magnetic Inv. in Geol & geophys inv. of Climax stock intrusive, NV USGS OFR 83-377, p. 40-77

East Mesabi IF.

Balsley, G.D., 1962, Geophys. re Iron Formations

$$M = kH = 0.108_{cgs} \times 0.590_e = 0.064 \text{ Gauss}$$

$$\left[1.0 \times 10^{-6} \times 10^{6} \times 10^{-6}\right]_{\mu cgs} = 0.064 \text{ Gauss}$$

Rosenbaum & Snyder

$$\vec{J}t = \vec{J}_r + \vec{J}_i = \vec{J}_r + \frac{k}{\mu_0}\vec{B}$$

$$\vec{J}_i = \frac{k}{\mu_0}\vec{B} = \frac{k\left[0.517 \times 10^{-4} T\right]}{\left[4\pi \times 10^{-7} Tm A^{-1}\right]}$$

@ $k = 1{,}000 \times 10^{-6}$ $\quad J_i = \dfrac{\left[10^{-3}\right]\left[0.517 \times 10^{-4}\right] T}{12.57 \times 10^{-7} Tm A^{-1}} = \dfrac{0.517}{12.57}$ A/m

$$J_i = 0.0411 \text{ A/m}$$

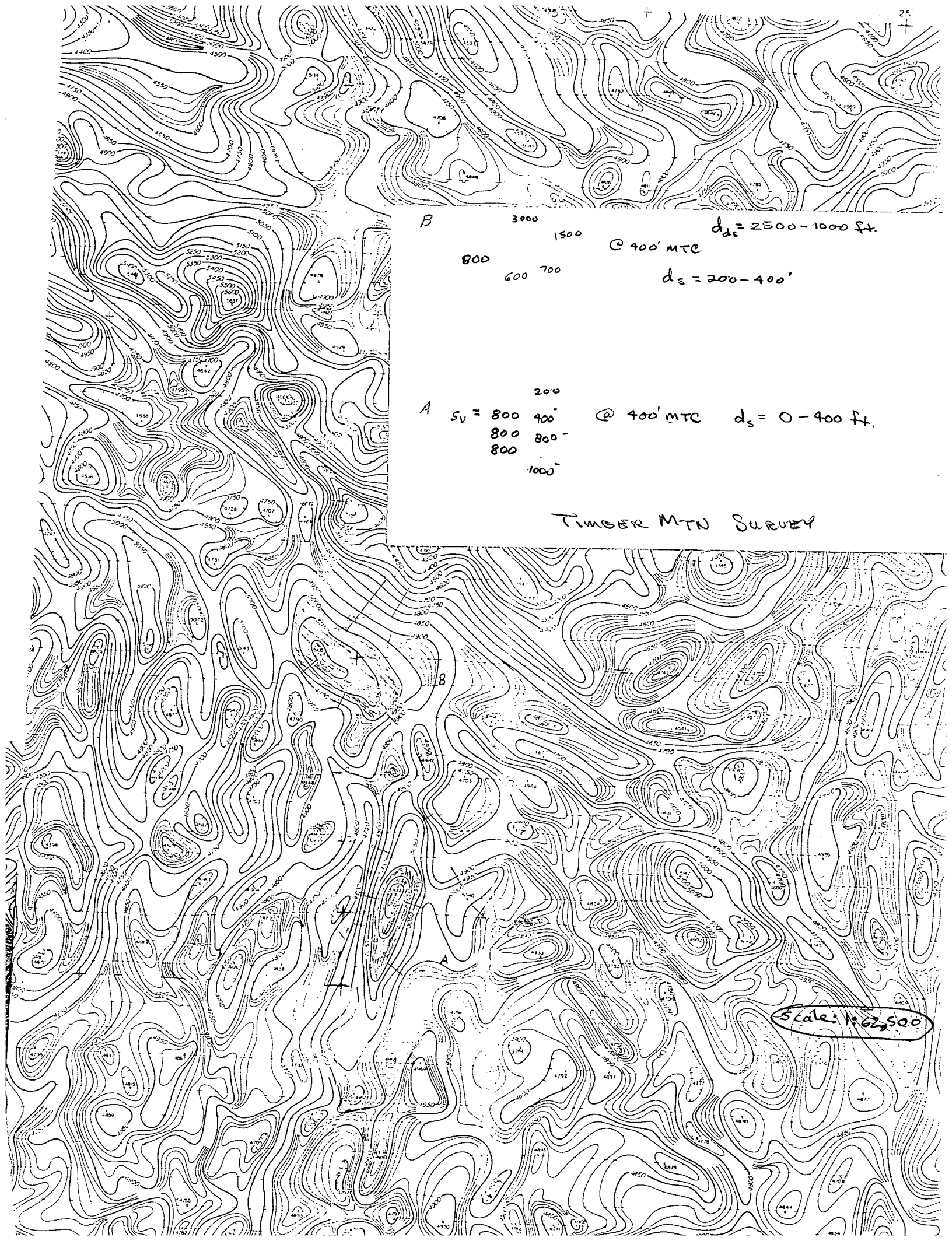
B
3000
1500
800
600
700
d_{ds} = 2500 - 1000 ft.
@ 400' MTC
d_s = 200 - 400'
A
S_V = 800
800
800
200
400
800
1000
@ 400' MTC
d_s = 0 - 400 ft.
TIMBER MTN SURVEY
Scale: 1:62,500

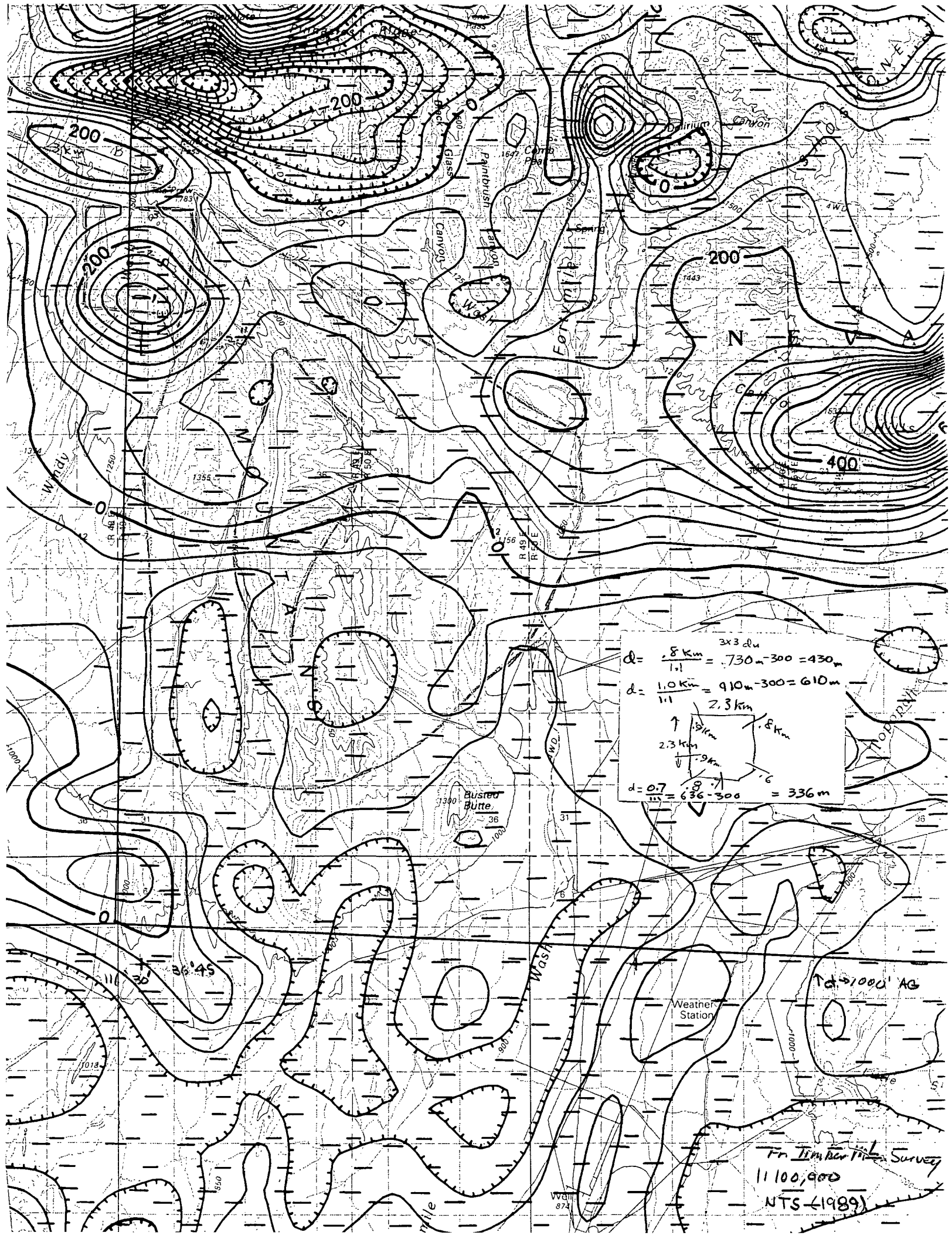
200
200
200
0
0
0
0
400
Delirium Canyon
Paintbrush Canyon
Fork
Canyon
Windy
Wash
Busted Butte
Weather Station
3x3 dw
d= .8 km / 1:1 = 730m - 300 = 430m
d= 1.0 km / 1:1 = 910m - 300 = 610m
2.3 km
.9 km
.8 km
.6
d= 0.7 / ... = 636 - 300 = 336m
Td → 1000' AG
Fr Timber Mtn Survey
1:100,000
NTS-(1989)

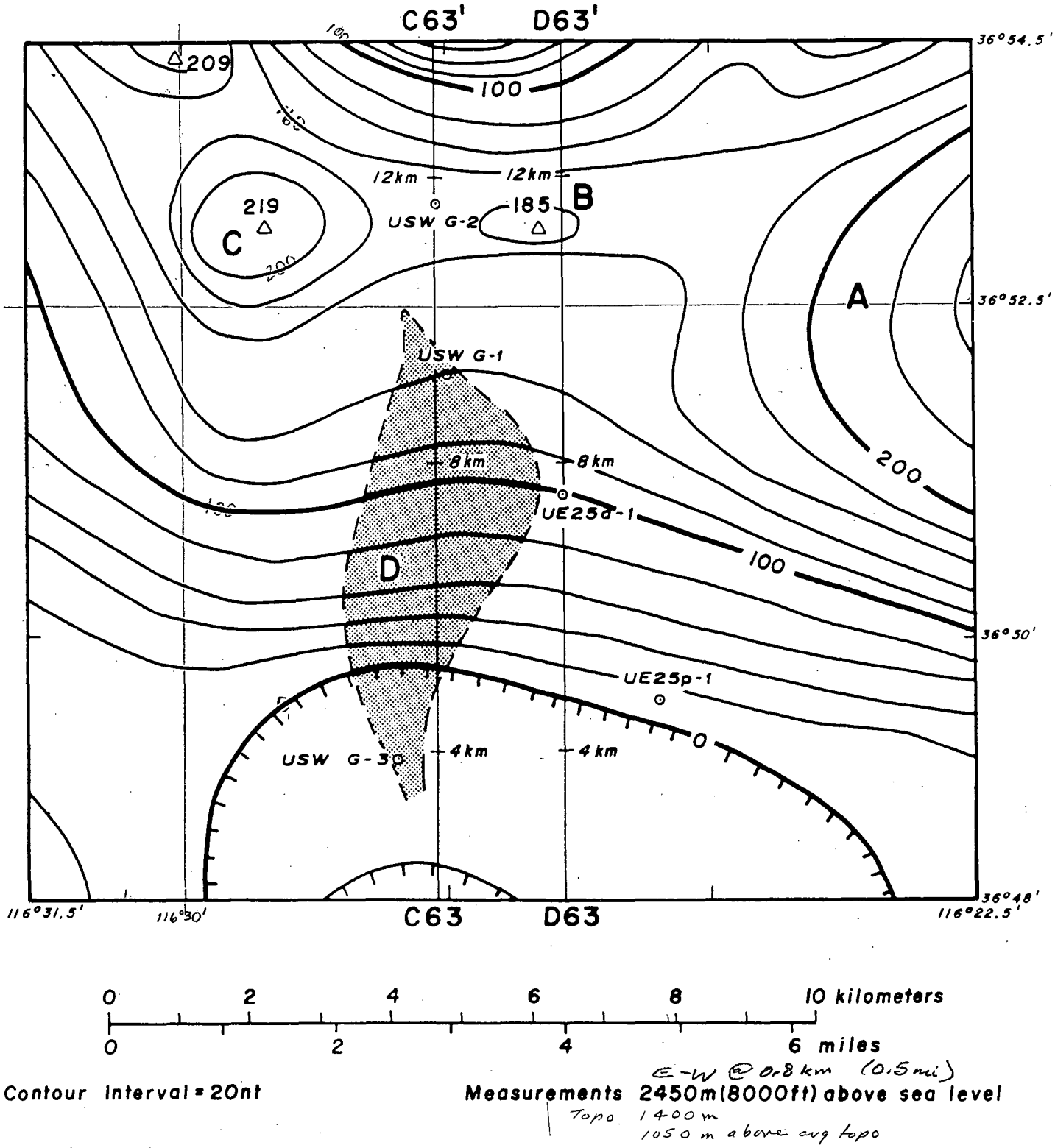

Figure 2.--Residual aeromagnetic map of Yucca Mountain area showing broad positive anomaly extending westward from A to maxima of 185 nT at B and 219 nT at C. Also shown are current (1983) proposed site area (shaded), parts of traverses C63-C63' and D63-D63', five drill holes, and the small change in spacing of contours over the site at D.

Anomaly Analysis

Almost all of the broad positive anomaly is assigned to effects of a deep source. The irregular patterns of positive and negative anomalies outlined in low-altitude surveys arise from a thick sequence of volcanic rock, but the anomalies tend to merge and cancel in surveys at high altitude. Exceptions are local anomalies from a few strongly magnetized units: the high of 185 nT near B, the high of 219 nT near C, and others. The cancellation is illustrated on figures 1 and 2 by values near zero over a typical sequence of volcanic rock along the southern part of the site. Also, the zero contours designate as nonmagnetic the thick pile of older sedimentary rocks beneath the volcanic rocks.

The KPQ inverse method indicates the large positive anomaly can be explained by a sheetlike source with its center at an elevation of -1,280 m (-4,200 ft) below sea level. The analysis was from data obtained along two long north-south profiles, C63-C63' and D63-D63', and shown as profiles on figures 4 and 5. The source extends in both the east-west strike direction and the north-south dip direction. It is designated sheetlike because the thickness is less than one-half the depth of 3.73 km (2.32 mi) beneath the air datum. The thickness is, therefore, too "thin" to be evaluated by this method.

The tabular model shown in section on figures 4 and 5 was determined by progressive modification of assumed models until a reasonable fit was found for anomalies observed, and anomalies calculated with a three-dimensional forward program. The source rock consists of magnetized Eleana Formation, and represents a westward extension of the rocks at Calico Hills. The magnetization is, therefore, normal with a total intensity of 3.89 A/m. The model is a rectangular vertical prism with its horizontal top at an elevation of -885 m (-2,900 ft). The prism is 14 km (8.7 mi) long east-west, 7.6 km (4.7 mi) wide north-south, and 825 m (2,700 ft) thick.

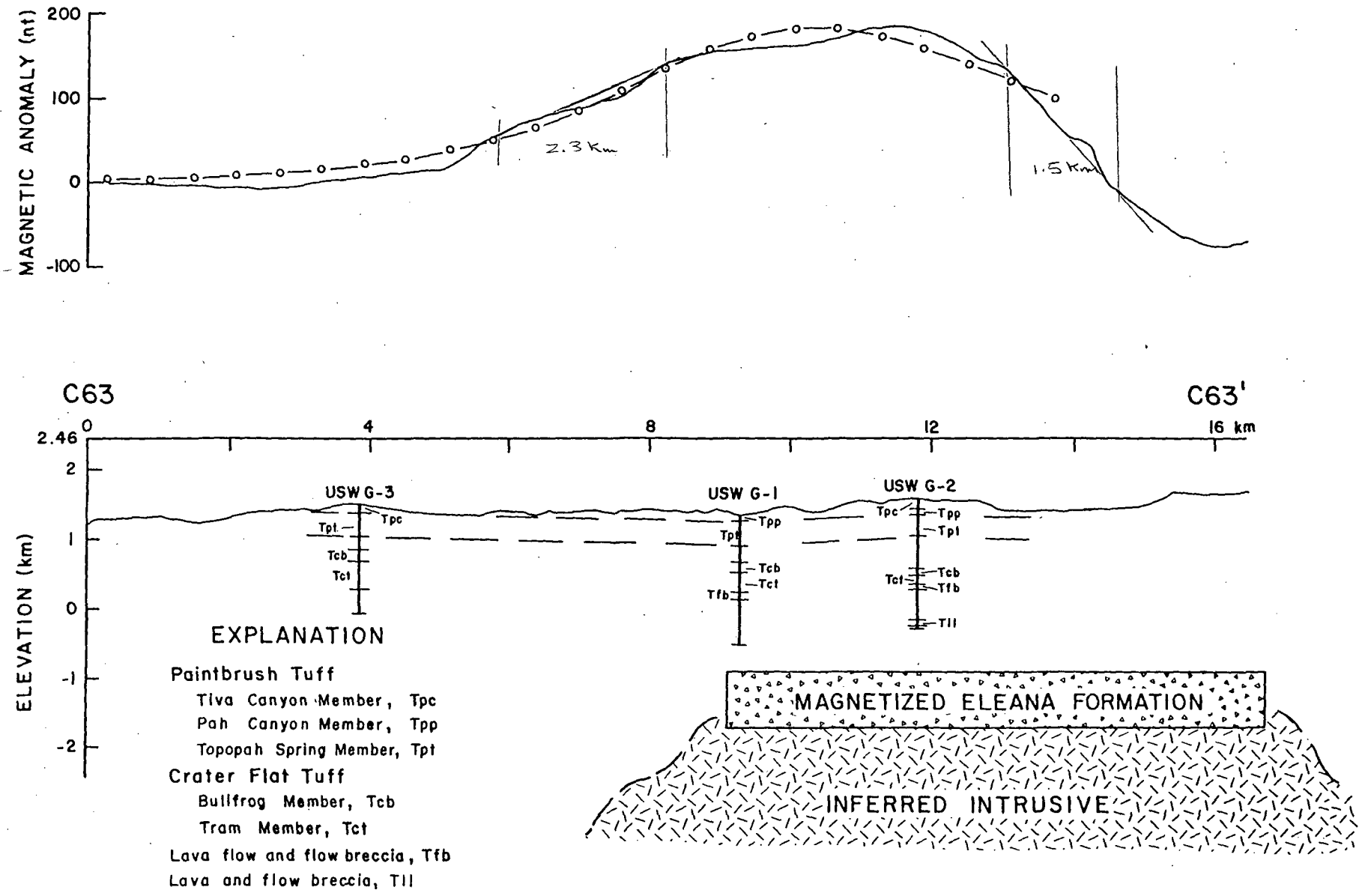

Figure 4.--Cross section along traverse C63-C63' and through the model of strongly magnetized Eleana Formation. Residual anomaly is solid line, and anomaly of model is line with values computed at circles. Also shown are the magnetized Tertiary volcanic units that were penetrated in drill holes USW G-3, USW G-1, and USW G-2.

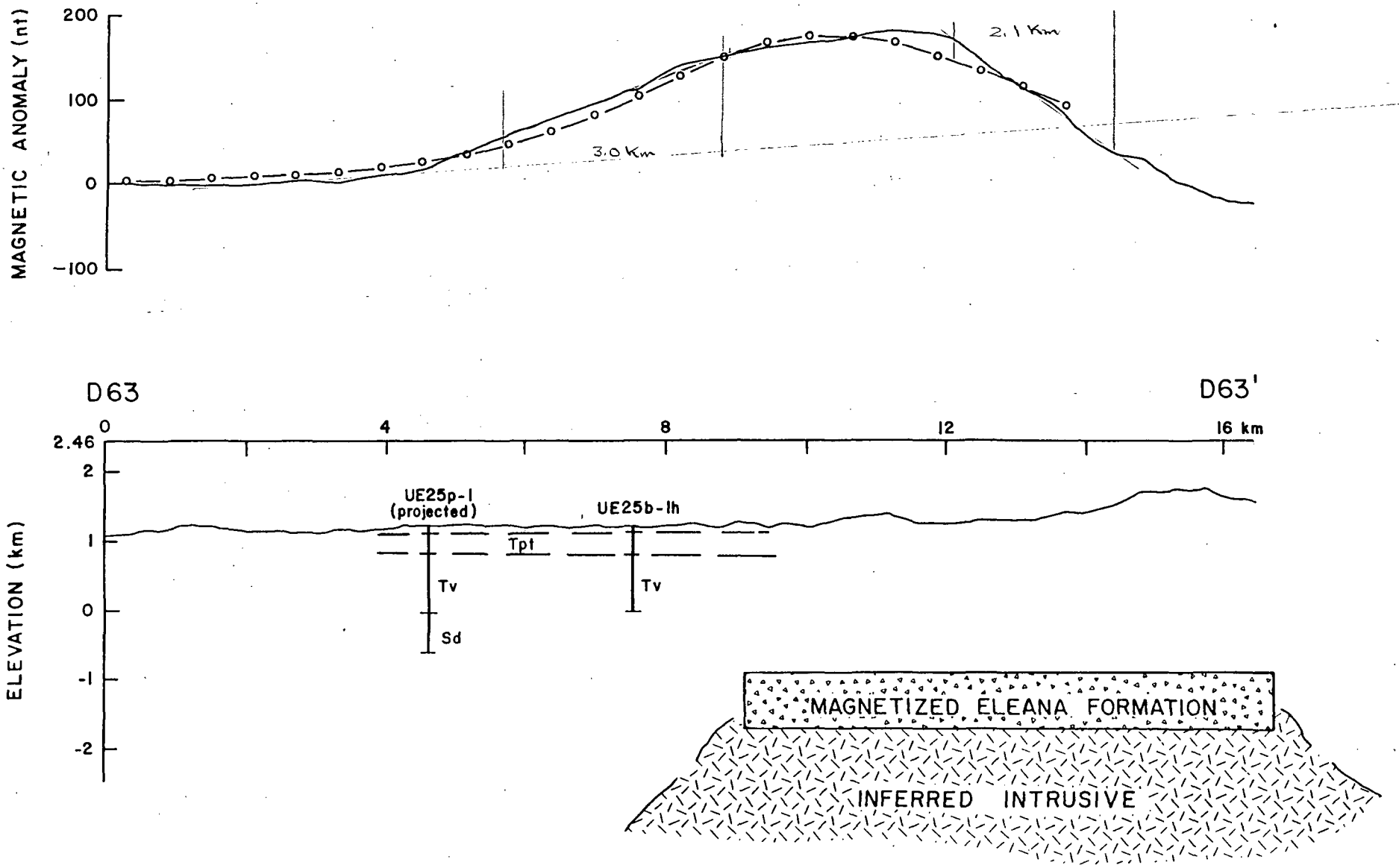

Figure 5.--Cross section along traverse D63-D63' and through the model of strongly magnetized Eleana Formation. Residual anomaly is solid line, and anomaly of model is line with values computed at circles. Also shown are the magnetized Tertiary volcanic units (Tpt and Tv) penetrated in drill hole UE25b-1h, and the magnetized Tertiary volcanic units (Tpt and Tv) and nonmagnetic Silurian dolomite (Sd) penetrated in drill hole UE25p-1.

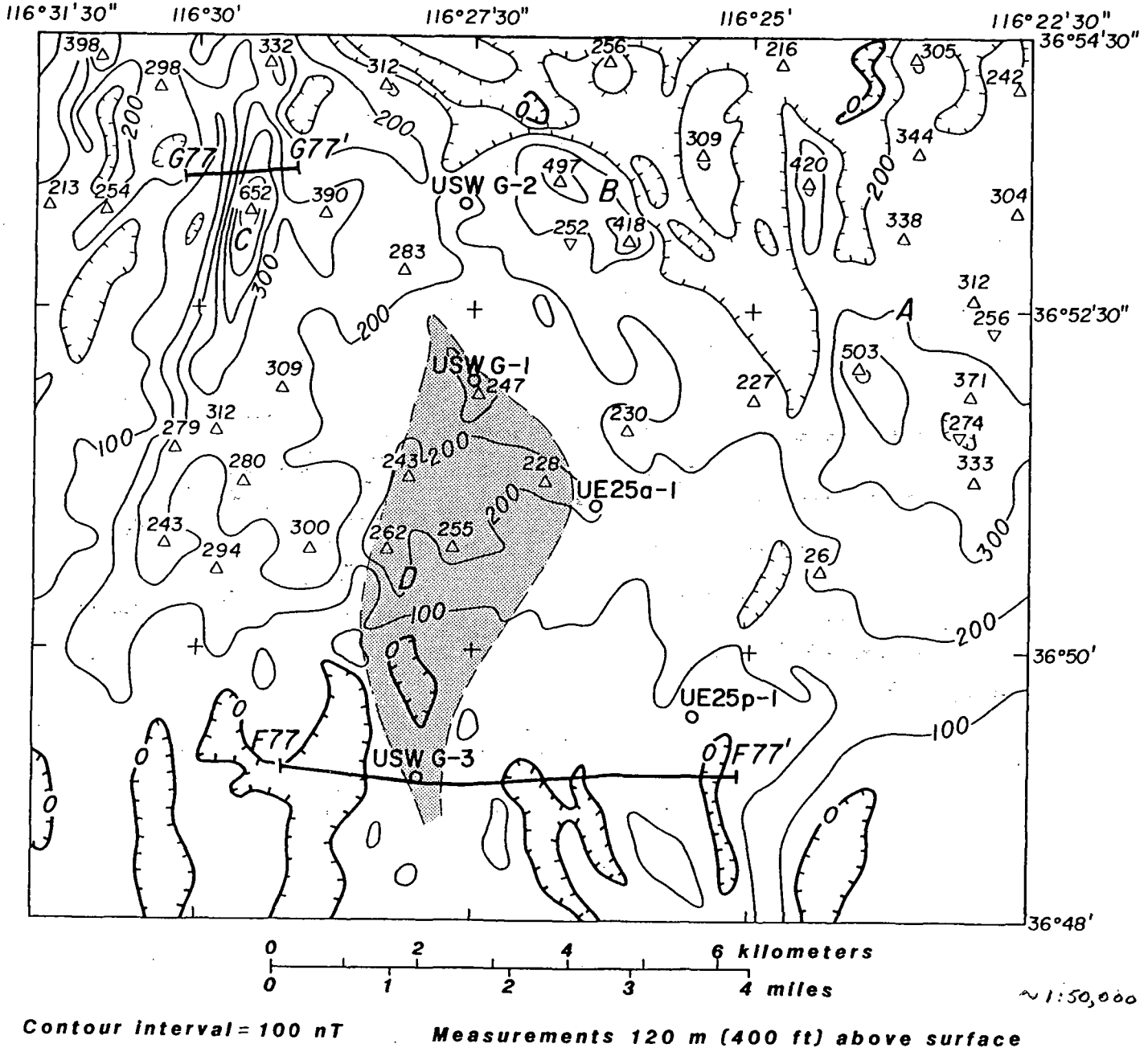

Figure 11.--Residual aeromagnetic map of Yucca Mountain area showing complex effects of volcanic rocks superimposed on deeper effects of magnetized sedimentary rocks. Also shown are the site area (shaded), areas A, B, C, and D of figure 2, air traverses F77-F77' and G77-G77', and five drill holes. Hachures indicate zero contours and closed areas of lower magnetic intensity.

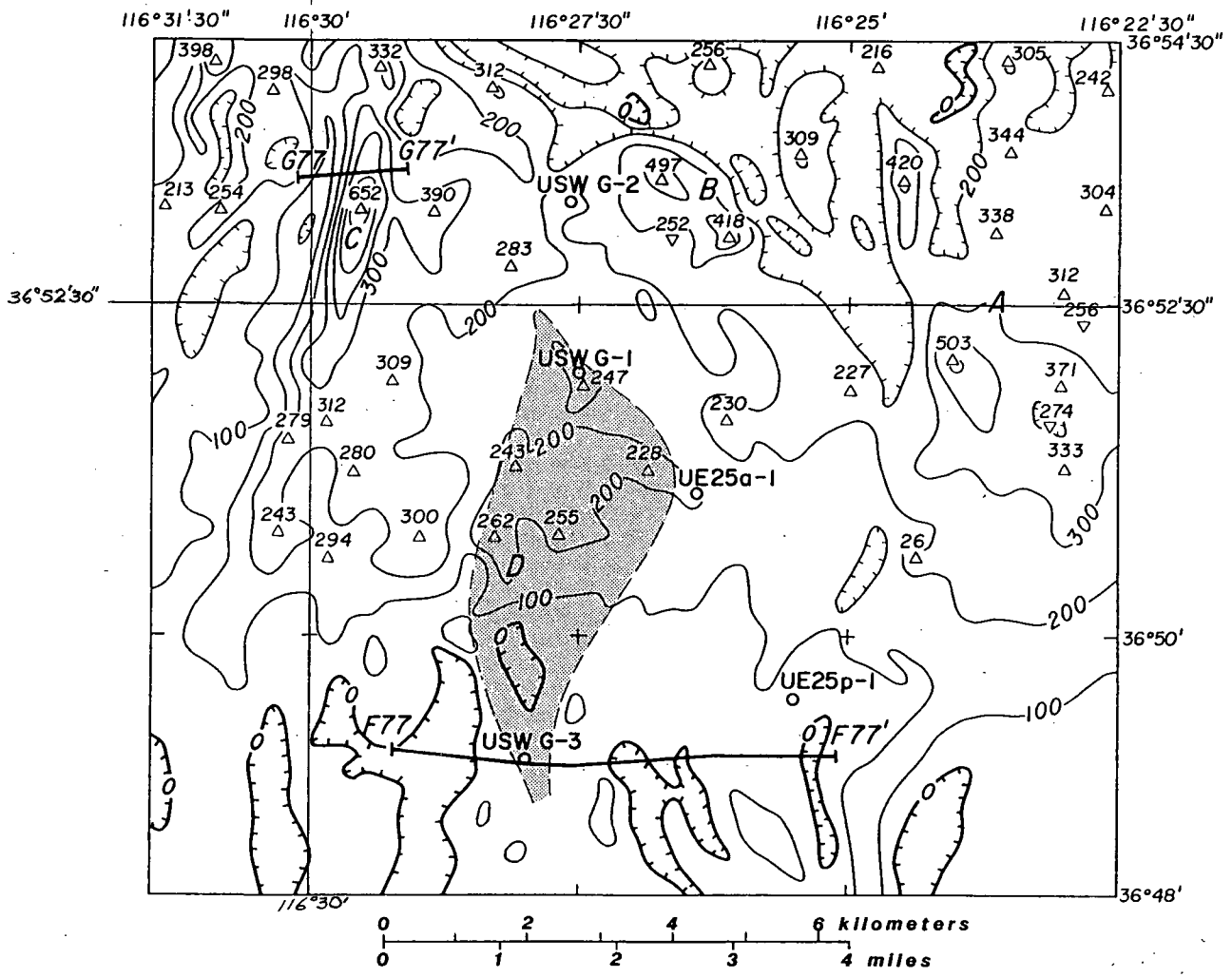

Figure 11.--Residual aeromagnetic map of Yucca Mountain area showing complex effects of volcanic rocks superimposed on deeper effects of magnetized sedimentary rocks. Also shown are the site area (shaded), areas A, B, C, and D of figure 2, air traverses F77-F77' and G77-G77', and five drill holes. Hachures indicate zero contours and closed areas of lower magnetic intensity.

Site Area @ 1:100,000

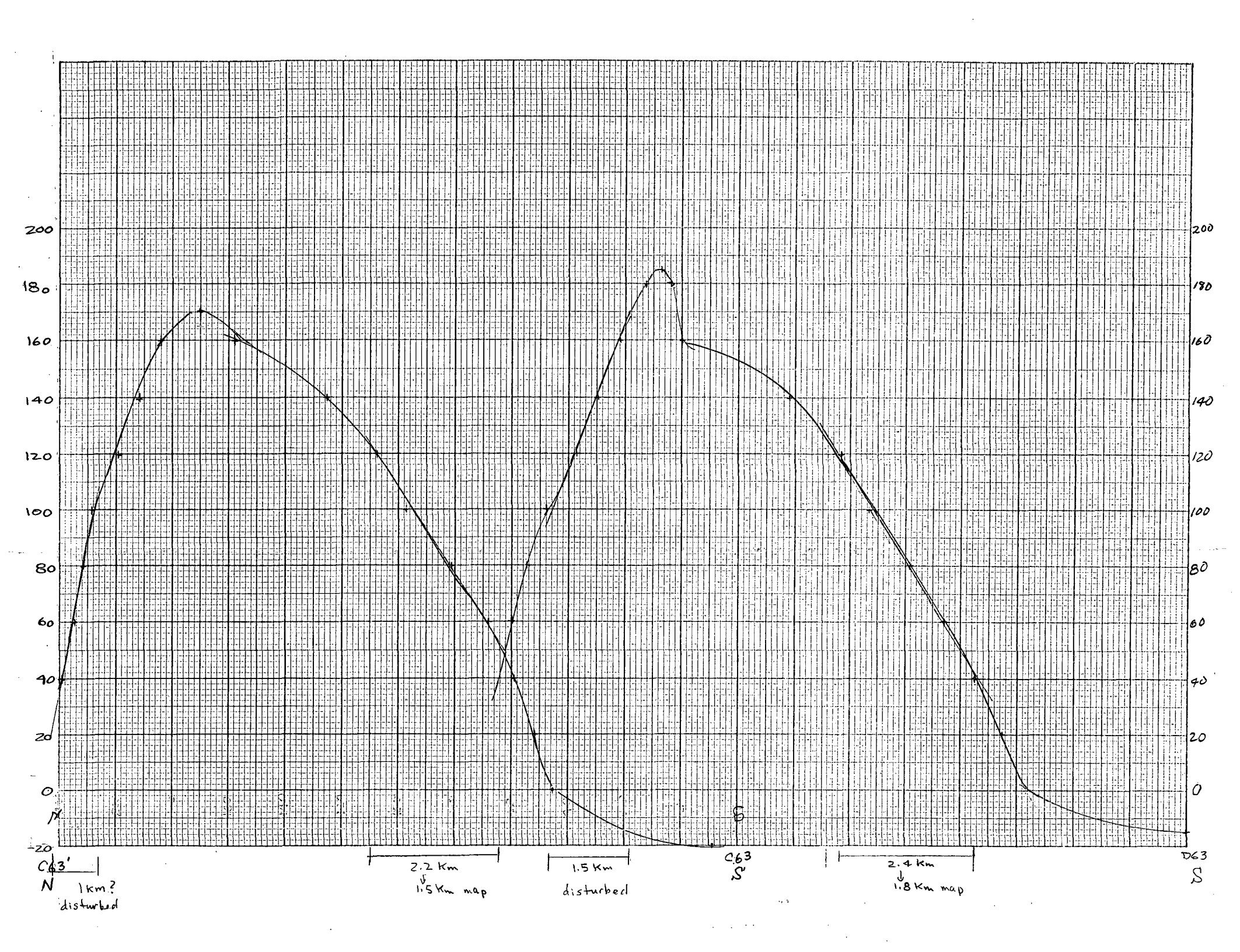
200
180
160
140
120
100
80
60
40
20
0
-20
C63'
N
1km?
disturbed
2.2 Km
1.5 Km map
1.5 Km
disturbed
C63
S
2.4 Km
1.8 Km map
D63
S

West Part of Calico Hills mag anomaly in YMCF-1 Depth Estimates:

Feighner and Majer: depths @ Peters Method, $d \sim S/1.6$

Profile Reg 2 & 3 (Crater Flat Anom. poor place angle)

Reg 2 @ N 60° E $d = \frac{12,245'}{1.6} = 7653' - 5000' = 2653'$ below surface

Reg 3 @ ~ E-W within Topopah Spring Tuff

A-A': N-S over Calico Hills: $d = 1125'$ F&M → Shallow magnetic tuffs; Ponce, Bath → Eleana Fm.

Bath & Jahren, 1984: Yucca Mtn Deep Source:

E-W traverses about 0.8 Km (0.5 mi) apart Elev = 2,450 m (8,000 ft.)

79/60: 20 cal

KPQ inverse method: Koulomzine et al (1970); Powell (1967) Qureshi and Nalaye (1978).

Interp by KPQ ⇒ sheetlike source w. center @ elev = -1,280 m (-4,200' b.s.l.)

p. 10 assumed sheetlike because the thickness is < 0.5 the depth of 3.73 km (2.32 mi) beneath the air datum

rectang. vertical prism, horiz. top @ E = -885 m (-2,900 ft)

14 Km (8.7) mi long E-W, 7.6 Km (4.7 mi) wide N-S, 825 m (2,700') thick

SS 4x6 : ∞ = N 0.8 / S 1.0 to 1.25

4x6 : 1 = 1.0 / 0.8

VACQUIER: $G_{(w)}$ 1.2, $E_{(s)}$ 1.3

C63': $\frac{2.2 \text{ km}}{1.3} = 1,692_m - 2,450_m = 758_{m.e}$ Alt

$\frac{1.5 \text{ Km}}{1.3} = 1,154_m - 2,450_m = 1,296_{m.e}$

Surface elev 1500 – 1250 m, 1400 m avg.

E $1450_m - 758_m = 692_m$ deep b.s.

$1,296_m - 1450_m = 104_m$ deep

D63: $\frac{2.4 \text{ km}}{1.3} = 1,846_m - 2450_m = 604_m$ Alt

$\frac{1.8 \text{ km}}{1.3} = 1,384_m - 2450_m = 1,065_m$

Elev = $1400_m - 604_m = 796_m$ b.s.

$1450_m - 1065_m = 385_m$ b.s.

$\frac{\text{Slope Indice}}{\text{True Depth}} = \frac{\text{Slope Dist map}}{\text{True Depth anom.}}$

$\text{True Depth}_{\text{anom}} = \frac{\text{Slope Dist map}}{\text{Slope Indice}} = \frac{X_{(m)}}{E, G\ (1.3)}$

Topopah Spring Anmag of Boynton, G.R. and Vargo, J.L, 1963

Flown @ BE @ 8000' Anomaly 116°30' 36°53" N

ΔS = 2000' - 5000' mag below plane = (-) 6000' elev to 3000' elev a.s.l.

topo elev = 4400' to 5000' + 4700' - 4700'
4700'
+1300' above ground to 1700 ft. deep.

Jan 27, '97

Magnetic Anomaly - NW YMCA

anomaly A — 1 km north of 36° 52' 30" @ 116° 30' 00"

NTS Map 1:100,000 : Kirchoff-Stern, Ponce and Churchel (1989)

* 280γ wrt @ 6 kg.

depths = _____

300 +215

* E-W flight lines, 400' AG, ¼ mi EW - 1:62,500

2808 on Timber Mtn Area survey, USGS 1977

NTS map - gridded @ 1 km interval, IGRF removed; upward cont to 1000'

- average diff in anomaly position is 0.4 km (normal)
- Lathrop Wells error inherent, but not sign. due to 1 km gridding.
- LW is S & E of this area:

① due to 1 km gridding

TIMBER MOUNTAIN SURVEY (1977): scale: 1:62,500

2-3 km inside W border of YMCA. N-S @ 400m (1300') spacing.

B — YUCCA MTN SURVEY: Bath & Jahren (1985)

+290 nT anomaly is 6 km SSE of 280 nT anomaly on NTS compil

and directly over SW part of proposed repository

topo + terrain effects + anom due to Solitario Canyon fault.
red t.c. over top opah Spr.

d ≥ 0.36 km mat below aircraft = 360 m : @ 122 m t.c. source is about 0 to 240 m deep in volcanics.

Bath & Jahren say about 300-400 ft deep. agree

122 m (400') AG. not detected earlier

Topopah Spring Quadrangle & Part of Bare Mtn Quad. Boynton & Vargo (1963)

BE @ 8000 ft; 1961; E-W lines @ 0.5 mi; but directly over area 290 nT does not occur

must be a thin, small source which attenuates fast 1/r³

Anomaly 280 nT NTS

both maxima shown w. about 1 km offset; about 255 to 275 nT vs 280

and 255-275 vs 220 nT

Magnetic Field — SI: nT — CGS: 1nT = 1gamma
Magnetization — A/m — 1 A/m = 10^{-3} gauss

see Rosenbaum & Snyder OFR-85-49

Magnetization - USGS - SI vs. c.g.s.

1 gauss = 10^{-4} T = 10^{5} nT
= 100,000 nT

MAGNETIC $k = M/H$

H = 51,700 nT

	1	2	3 FIELD 51,700nT	4 & $\frac{A/m}{.517\times10^{-4}T}$	5	6 k_{cgs} emu/cm^3	7 k_{cgs} $\mu_{cgs}=10^{-6}$	8	9	
1			0.51700	Oe ($\times10^{-6}$)						
USGS defn 2	J_t (magnet) A/m									
non magnetic 3	0-0.05			0-967 ✓			0-77 ✓			
weakly magn. 4	0.05-0.50			967-9,671			77-770			
moderat. mag. 5	0.50-1.50			9,671-29,014			770-2,309			
6	1.00			19,342		10^{-3}	1,539			
strongly mag 7	71.50		↓	>29,014			>2,309			
8										
9										
10	1.0 A/m		(10^4 Oe) 1.0 T		10^4 Oe 10,000	10^{-3} emu/cm^3	1,000			
11										
12										
13		↓ After Rosenbaum & Snyde				→				
14	J_i (A/m)		T 0.517×10^{-4}	k (SI) ($\times10^{-6}$)		k (cgs) emu/cm^3 $\times10^{-6}$				
non-mag 15	0.000411			10		0.80				
non-mag 16	0.00411			100		7.95				
non-mag 17	0.0411			1,000		79.58				
0.05										
weakly mag 18	0.411			10,000		795.8				
0.50										
moderat. mag 19	0.822			20,000		1592				
" 20	1.233			30,000		2,388				
1.50										
strongly mag 21	1.644			40,000		3184				
strongly mag 22	4.110			100,000		7,958				
23										
24										
25										
Climax Stock NTS 26	J_i 0.15 A/m	@ surface								
" " 27	1.55 A/m	@ >700m								
28										
29										
30										
31										

Quantity	SI unit	Equiv. Unit (in emu)
Magnetic Field	nanotesla (nT)	1 nT = 1 gamma
Magnetization	ampere/meter (A/m)	1 A/m = 10^{-3} gauss
Magnetic Field	10^{-4} tesla	= 1 gauss